AKARI mission and calibration

Issei Yamamura (ISAS/JAXA)

on behalf of AKARI Project

Contributions:

S. Takita, S. Matsuura, M. Shirahata, S. Makiuti (ISAS),

Y. Doi (Univ. of Tokyo)

http://www.ir.isas.jaxa.jp/AKARI/

Alberto Salama

First visit to ISAS, 2002

Giving a speach at the banquet of AKARI conference, 2009

ASTRO-F Observing preparation workshop at ESAC, 2005

Thank you very much!

Outline of this presentation

- The AKARI mission
- The FIS instrument
- FIS All-Sky Survey (Point Source Catalogue) Calibration
- FIS image map calibration
- FIS Slow-scan calibration
- Pointing calibration
- Future

AKARI-FIS Bright Source Catalogue Ver.1

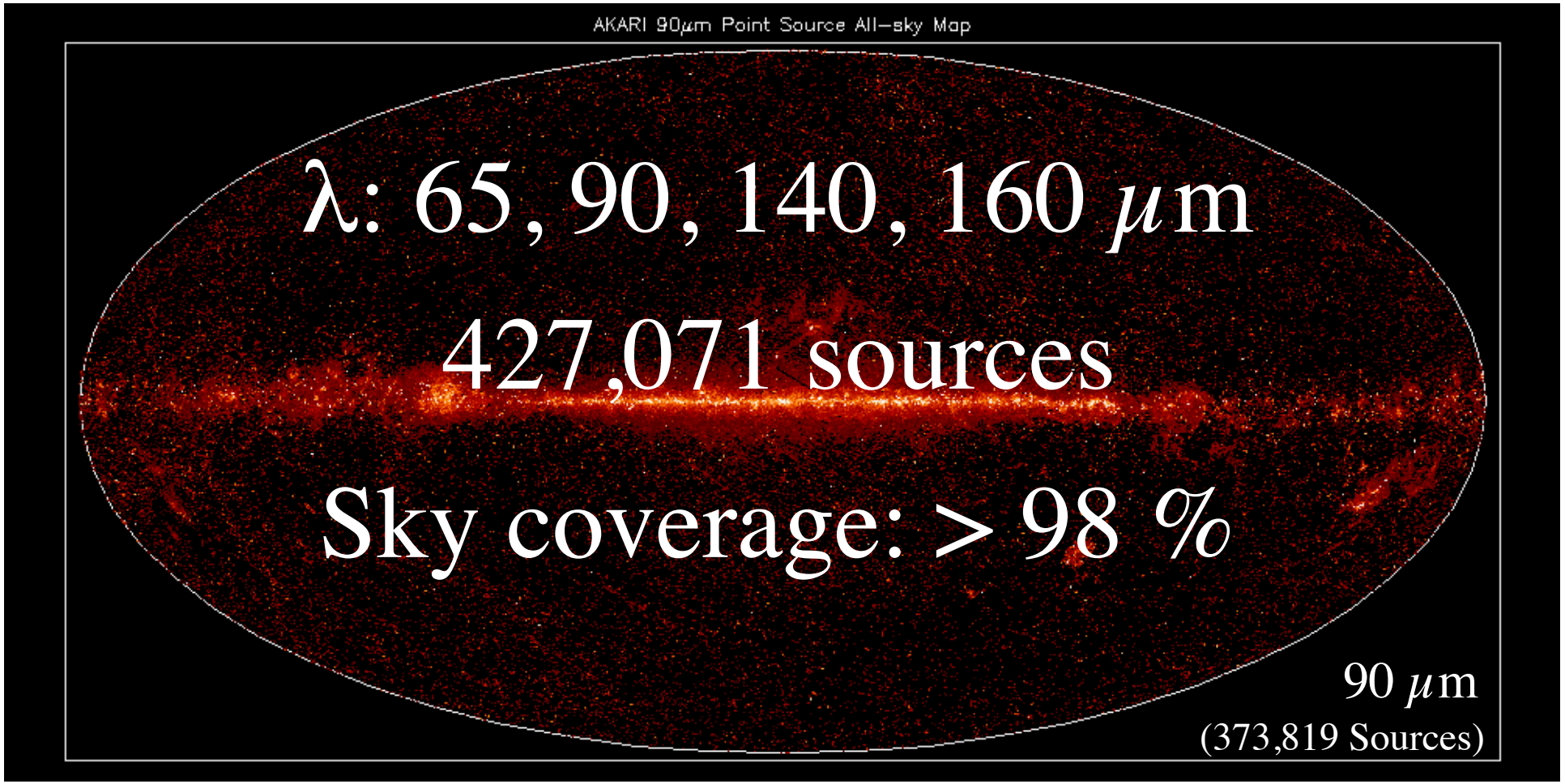

Far-IR All-Sky Image maps

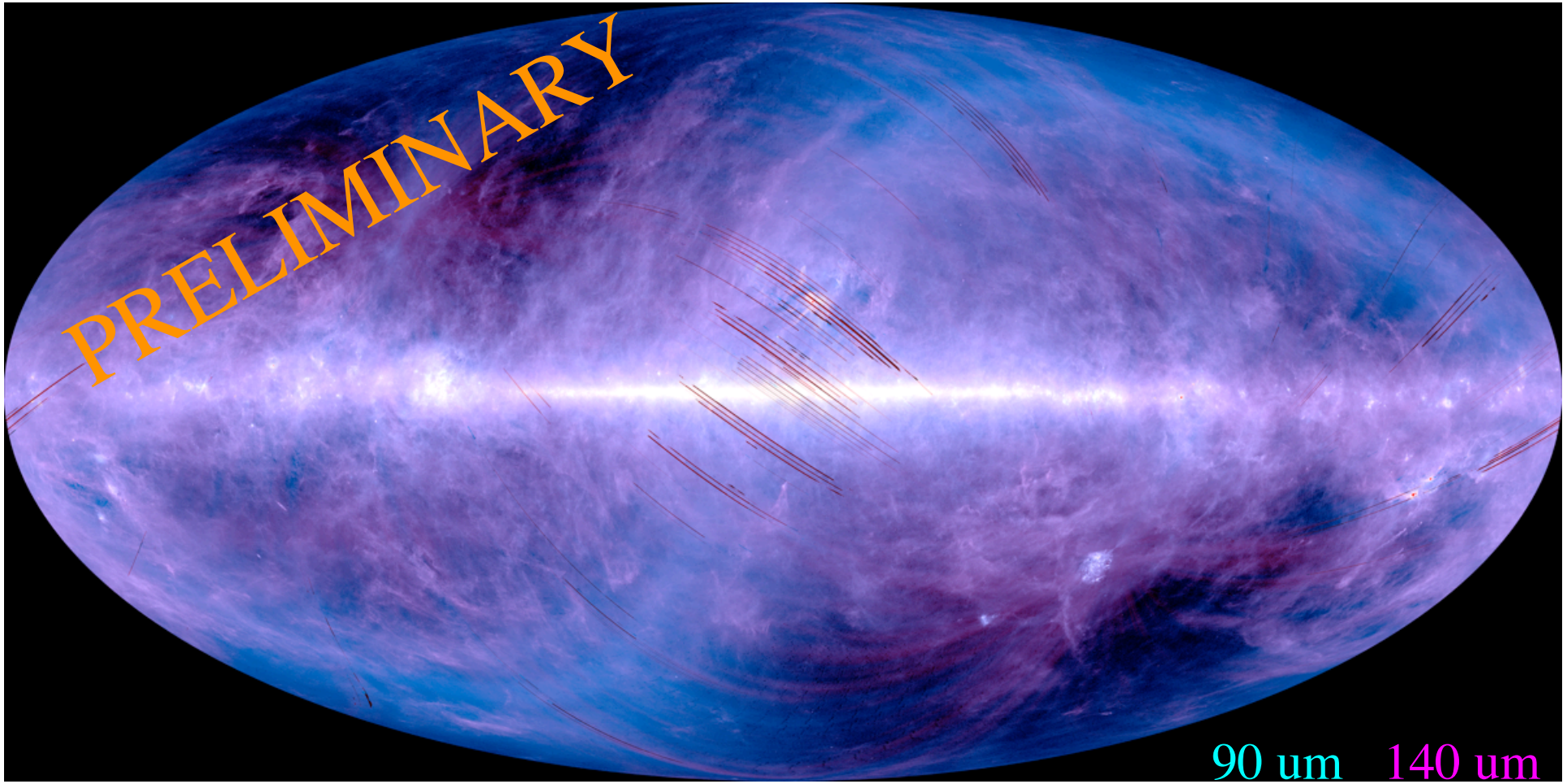

Far-IR mapping of the AKARI Deep Field South

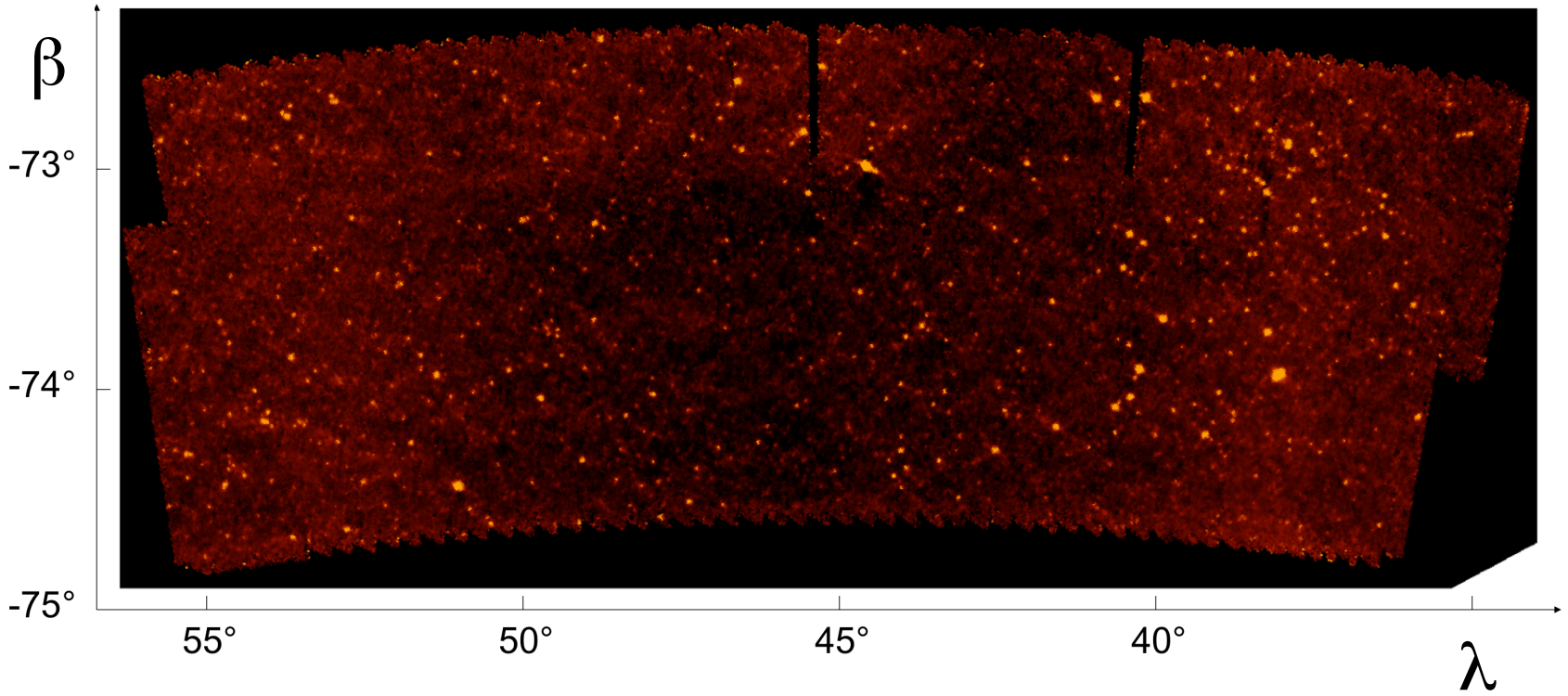

90 μm

Matsuura et al., 2011, ApJ 737, 2

AKARI Calibration papers

- FIS instrument flight performance
  Kawada, M., et al., 2007, PASJ 59, S389
- Slow-scan mode calibration
  Shirahata, M., et al., 2009, PASJ 61, 737 (Point source)
  Matsuura, S., et al., 2011, ApJ 737, 2 (Diffuse radiation)
- FIS-FTS Spectroscopy mode calibration
  Murakami, N., et al., 2010, PASJ 62, 1155
- AKARI-FIS Bright Source Catalogue Ver.1 Release note
- AKARI-IRC Point Source Catalogue Ver.1 Release note
  http://www.ir.isas.jaxa.jp/AKARI/Observation/PSC/Public/
- AKARI-IRC Point Source Catalogue Ver.1
  Ishihara, D., et al., 2010, A&A 514, A1
- IRC Image calibration
  Tanabe, T., et al., 2008, PASJ 60, S375
- IRC Slow-scan observation
  Takita, S., et al., 2012, PASJ 64, 126

The AKARI Mission

AKARI Satellite

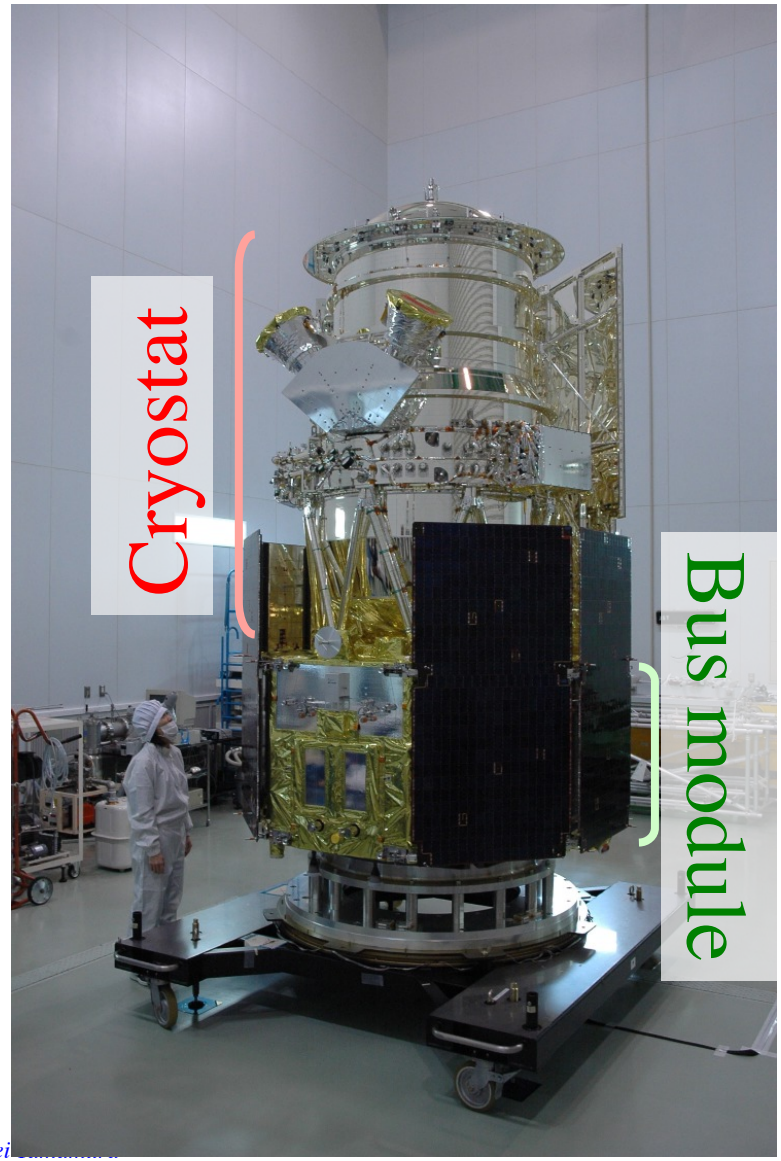

Height: 3.7 m

Weight: 952 kg (@Launch)

A 68.5 cm ϕ cooled telescope

Two scientific instruments covers wavelength in 1.8~180 μm

The telescope and focal-plane instruments were kept in 2~6 K by stirling coolers and liquid Helium

Orbit and Operation Modes

- Sun-synchronous polar orbit
- Altitude: 700 km
- Orbital Period: 100 min

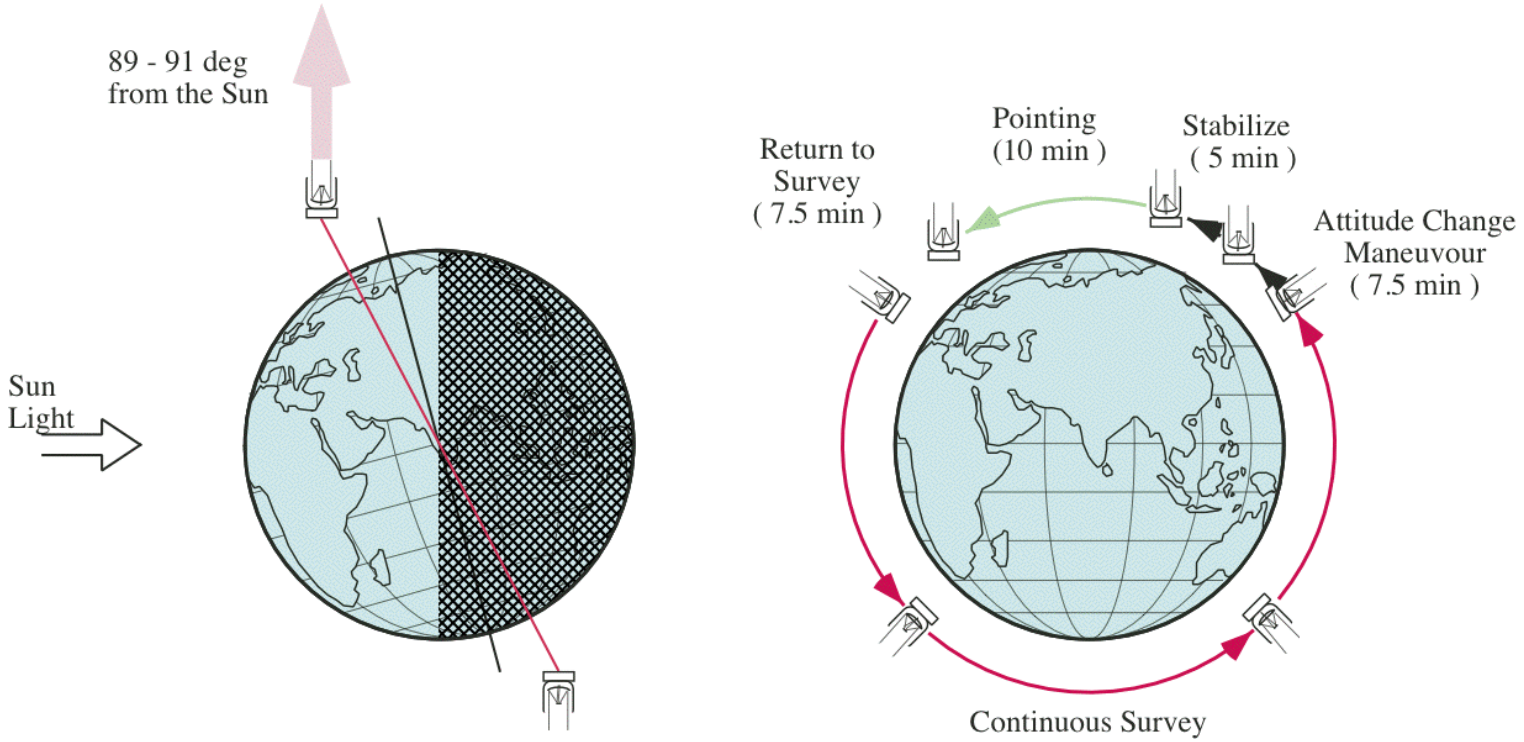

Survey Mode & Pointing Mode

Telescope & Instruments

- ϕ 685 mm, F/6.1, Ritchey-Chretien
- Silicon carbide mirror

50–180 μm

(Far-Infrared Surveyor) FIS

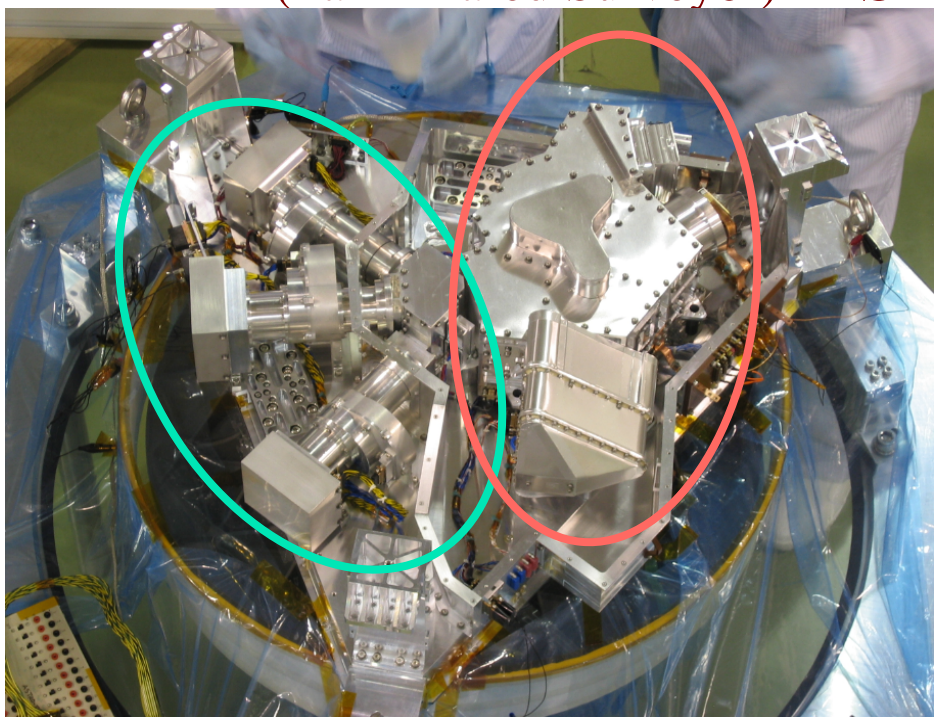

IRC (Infrared Camera)

1.8–26 μm

Onboard Instruments

Photometric & Spectroscopic Capabilities

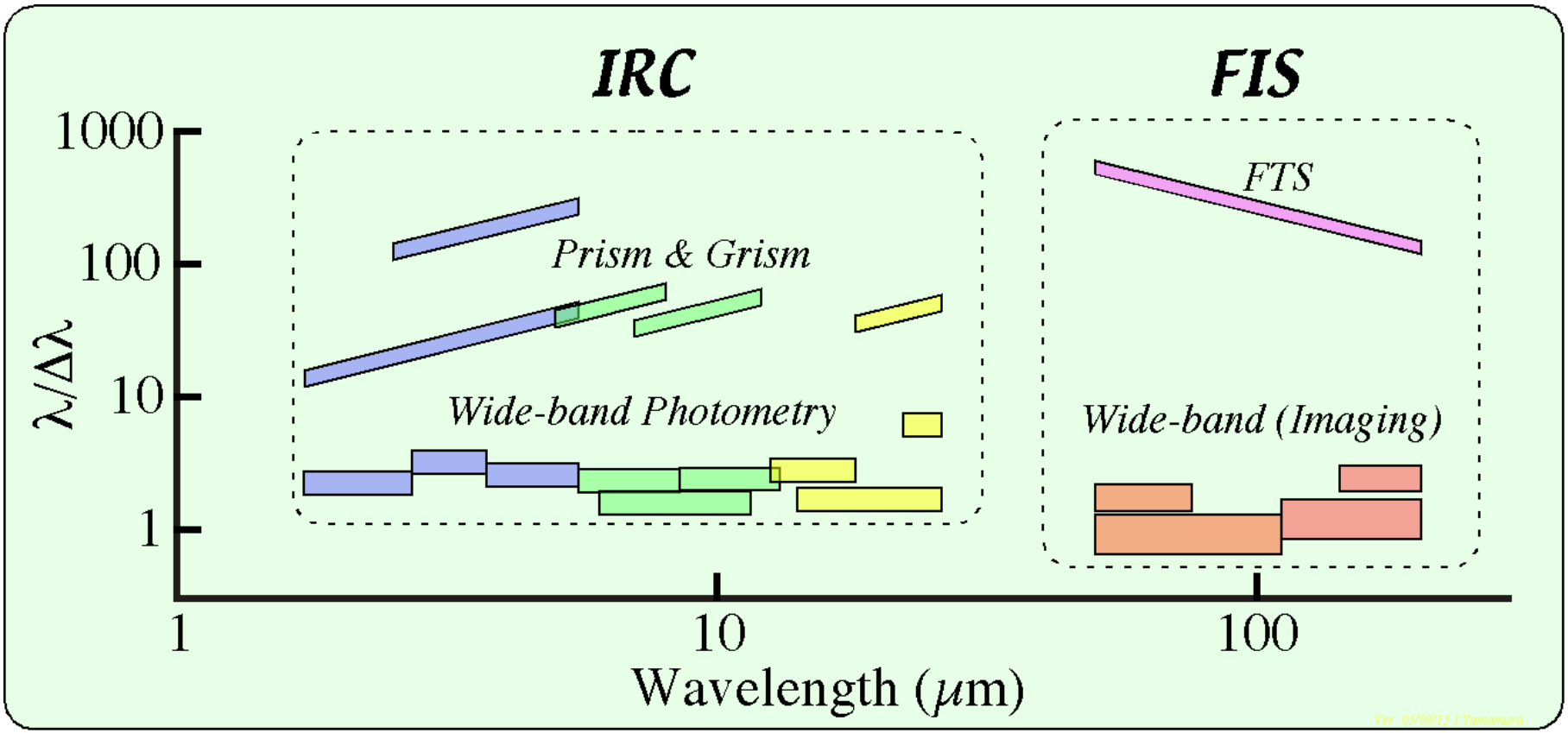

AKARI Operation history

Feb. 21, 2006 Launch	
Apr. 14, 2006 Ap.Lid Open	
Checkout	Checkout & Performance Verification
May 7, 2006	
Phase 1 (~180 days)	(FIS) All-Sky Survey: 1st priority LS+Some MP Pointed Obs
Nov. 10, 2006	
Phase 2 (~300 days)	MP + OT Pointed Obs. Supplemental (FIS) survey
Aug. 26, 2007 LHe boil-off	He holding time 550 days
2nd PV	
June 1, 2008	
Phase 3	only NIR in operation MP + OT pointed Obs.
Feb. 15, 2010	
Maintenance	Cryo-cooler degradation/recovery
Nov. 24, 2011 Satellite power-off	

AKARI Catalogues

Catalogue	Release date	# of sources	Description
AKARI-FIS Bright Source Catalogue ver.1	2010/03/30	427,071	Sources observed at 65, 90, 140, 160 μm from the All-Sky Survey
AKARI-IRC Bright Source Catalogue ver.1	2010/03/30	870,973	Sources observed at 9 & 18 μm from the All-Sky Survey
The AKARI Asteroid Catalogue ver.1	2011/10/14	5,120	Diameter and albedo of asteroids observed in the IRC All-Sky Survey
AKARI LMC Point Source Catalogue ver.1	2012/11/13	660,286	Sources observed in the LMC region of 10 deg^2 at 3, 7, 11, 15, 24 μm
AKARI LMC Near-Infrared Spectroscopic Catalogue ver.1	2013/01/07	1757	Spectra of sources in the LMC survey region in 2.5–5.0 μm
The AKARI NEP-Wide Source Catalogue ver.1	2013/03/15	114,794	Sources detected in the North Ecliptic Pole region of 5.4 deg^2 observed at 2, 3, 4, 7, 9, 11, 15, 18, 24 μm
The AKARI NEP-Deep Source Catalogue ver.1	2013/03/15	7,284	Sources detected in the North Ecliptic Pole region of 0.67 deg^2 observed at 2, 3, 4, 7, 9, 11, 15, 18, 24 μm. 2–3 time deeper than the NEP Wide catalogue

The FIS instrument

FIS Photometric Mode

Band	N60	WIDE-S	WIDE-L	N160	
Wavelength	50–80	60–110	110–180	140–180	[μm]
Central Wavelength	65	90	140	160	[μm]
Detector	Monolithic Ge:Ga		Compact Stressed Ge:Ga		Ge:Ga chips supplied by NICT
Readout	Charge Trans-Impedance Amplifier (CTIA)				
Array format	20 x 2	20 x 3	15 x 3	15 x 2	Pixels
Pixel size (Physical size)	27 x 27 (0.5 x 0.5)	27 x 27 (0.5 x 0.5)	44 x 44 (0.9 x 0.9)	44 x 44 (0.9 x 0.9)	[arcsec^2] ([mm^2])

FIS Detectors

WIDE-S: 3x20

N60: 2x20

N160: 2x15

WIDE-L: 3x15

Overlap each other

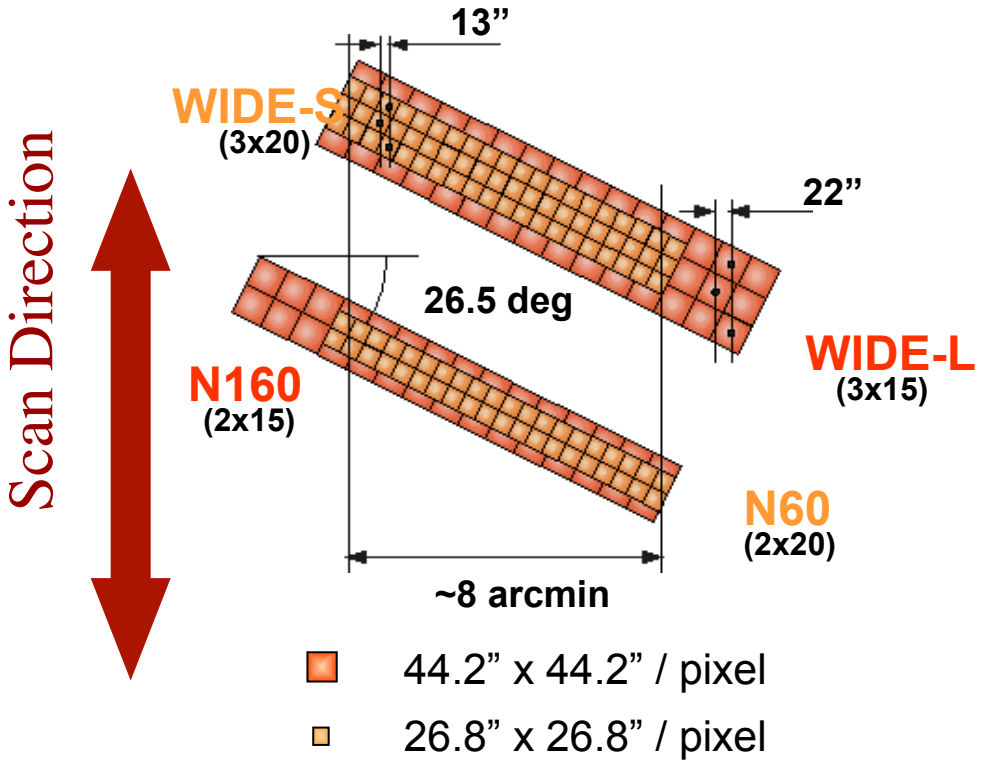

FoV of the FIS

Scan direction ~ along the constant Ecliptic longitude

FIS RSRF

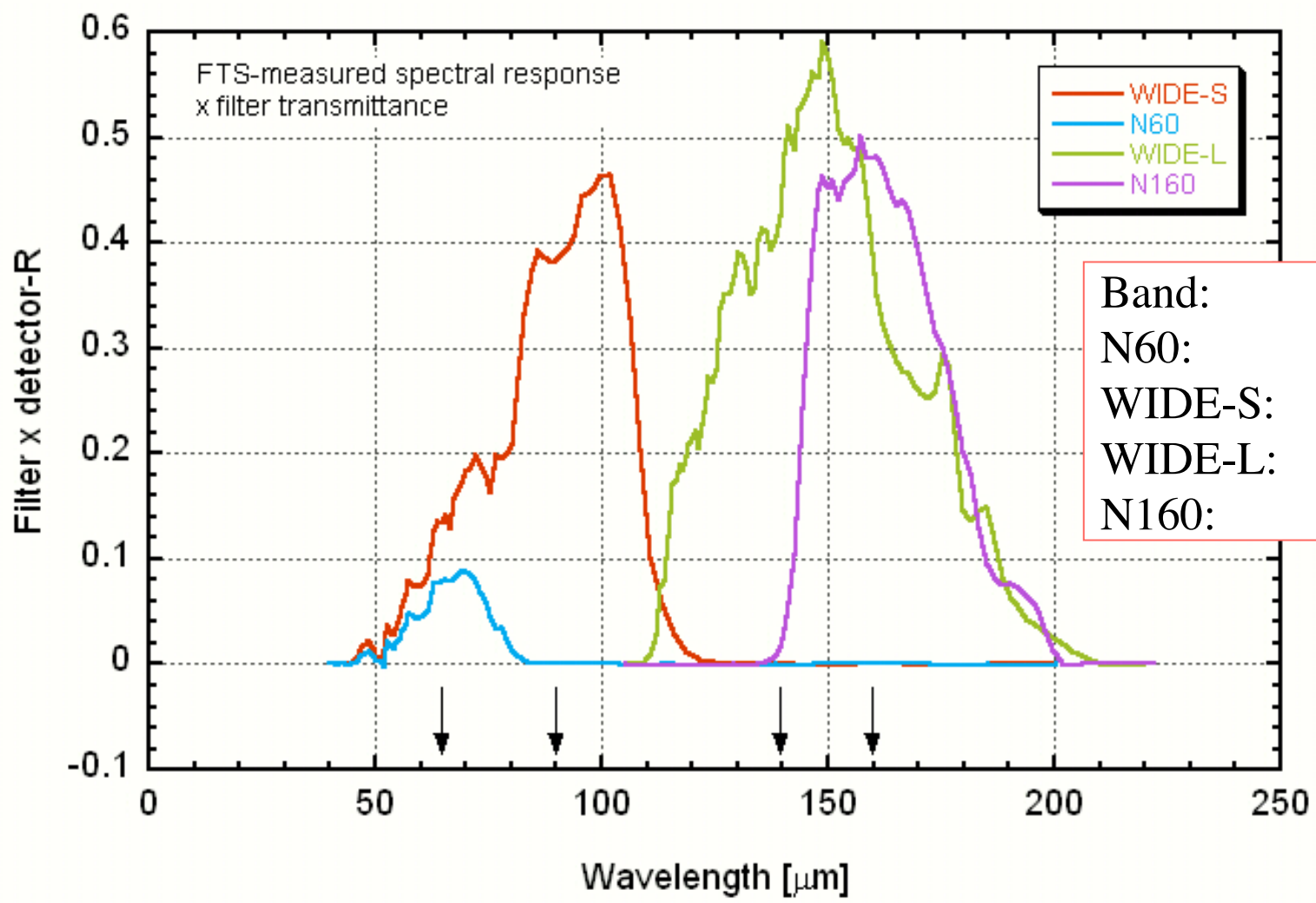

Band:	λc
N60:	65 μm
WIDE-S:	90 μm
WIDE-L:	140 μm
N160:	160 μm

Data acquisition modes (Photometry mode)

Sampling rate

SW:~24 Hz, LW:~16 Hz

(A) 6-Averaging sampling

Nominal mode

for photometry

The SW and LW detectors are reset simultaneously

Reset interval: 0.5 sec, 1 sec, 2 sec

(B) Differential sampling / CDS

higher saturation level

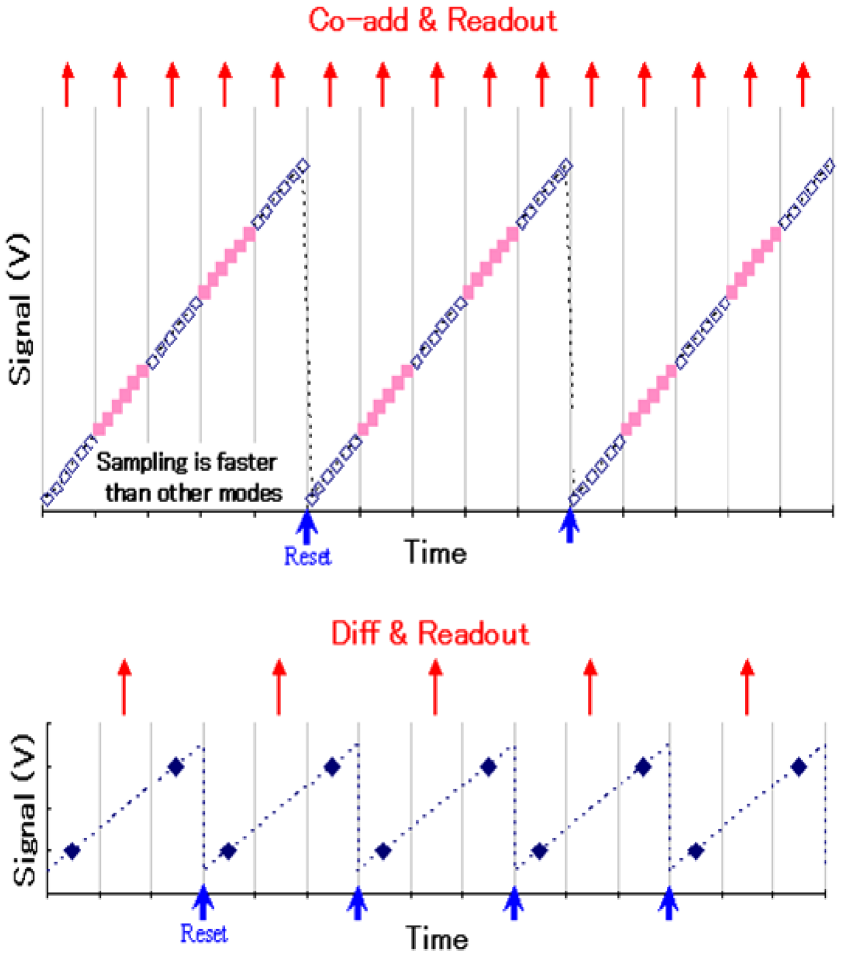

FIS internal calibration source

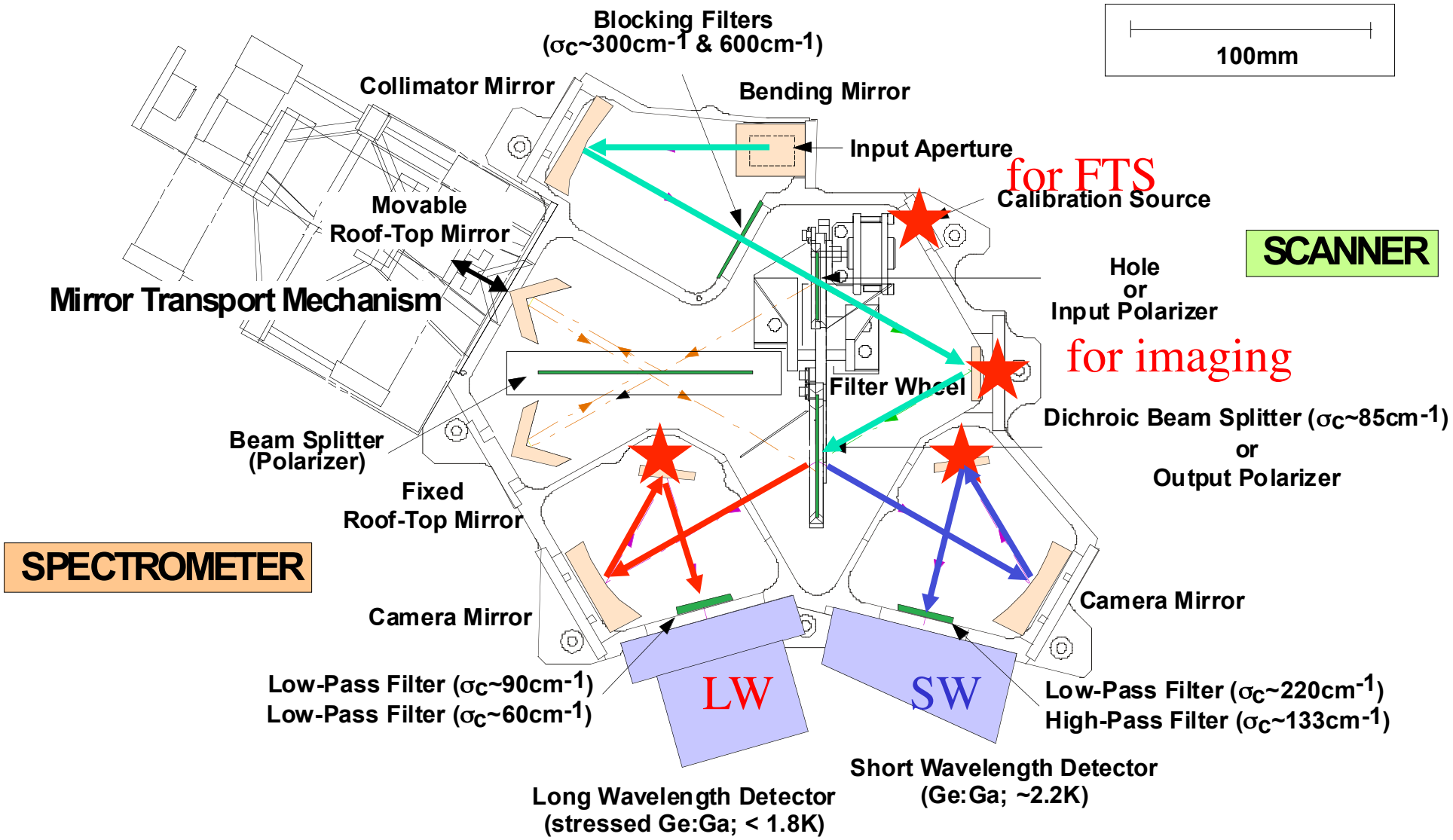

The FIS All-Sky Survey Calibration

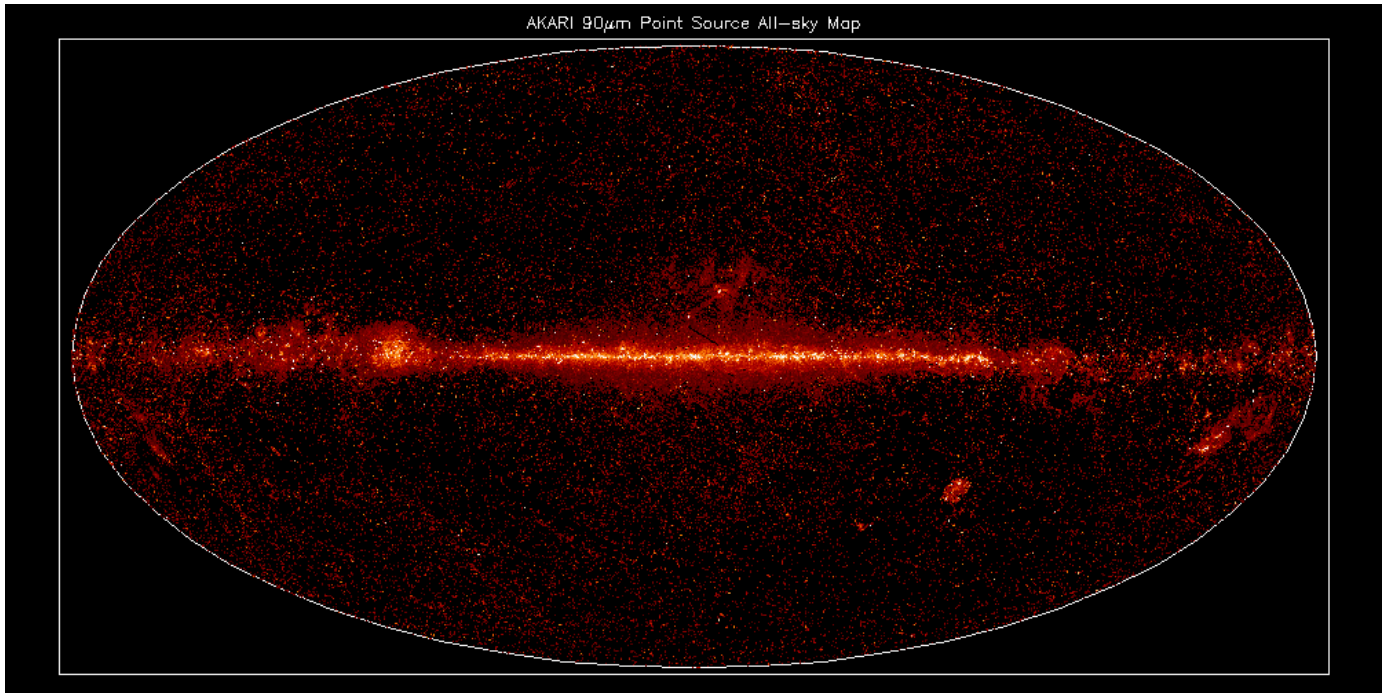

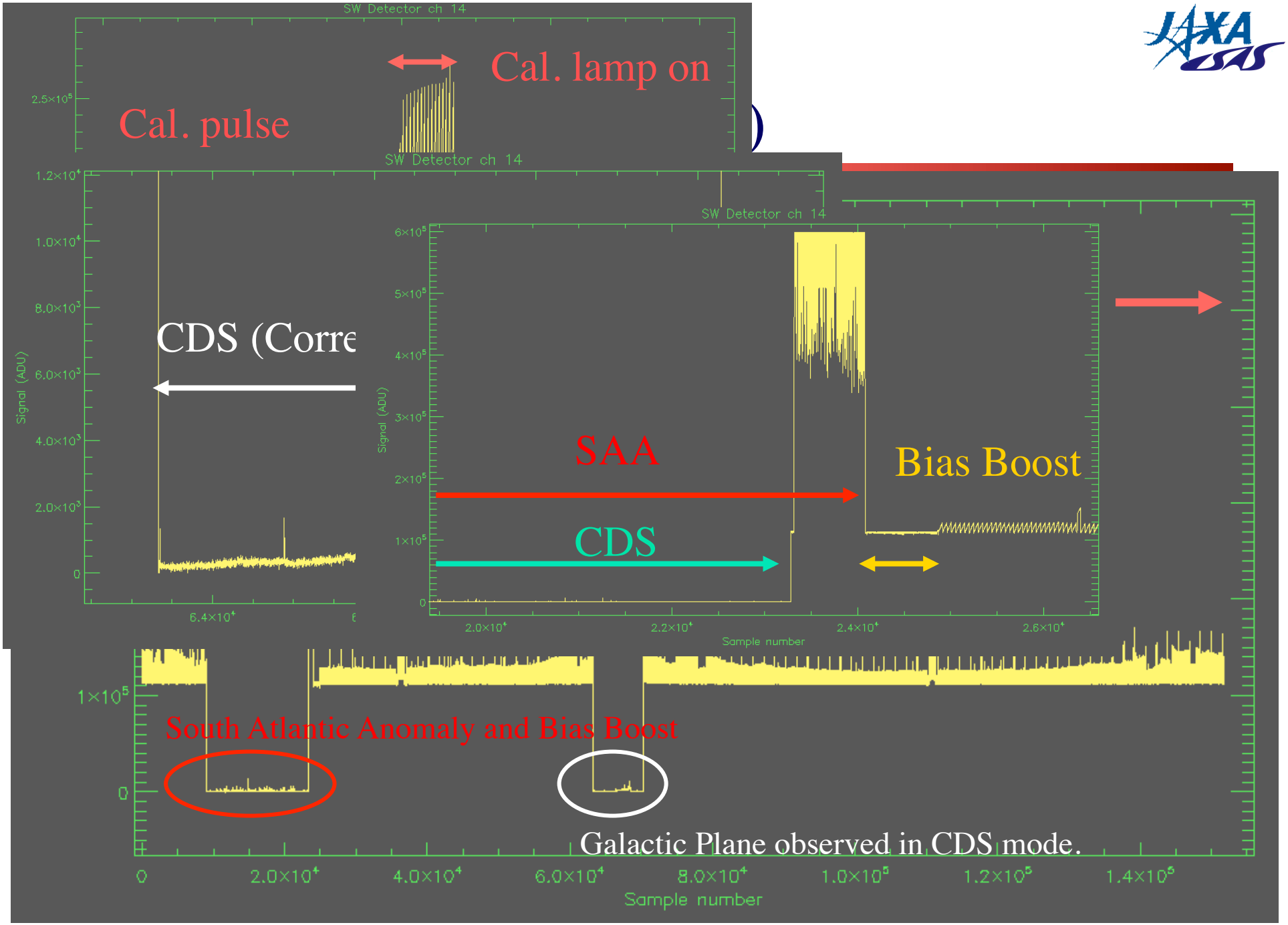
SW Detector ch 14
Cal. lamp on
Cal. pulse
SW Detector ch 14
SW Detector ch 14
CDS (Corre
Signal (ADU)
SAA
Bias Boost
CDS
Sample number
South Atlantic Anomaly and Bias Boost
Galactic Plane observed in CDS mode.
Sample number

Green Box: correction/calibration of time series data

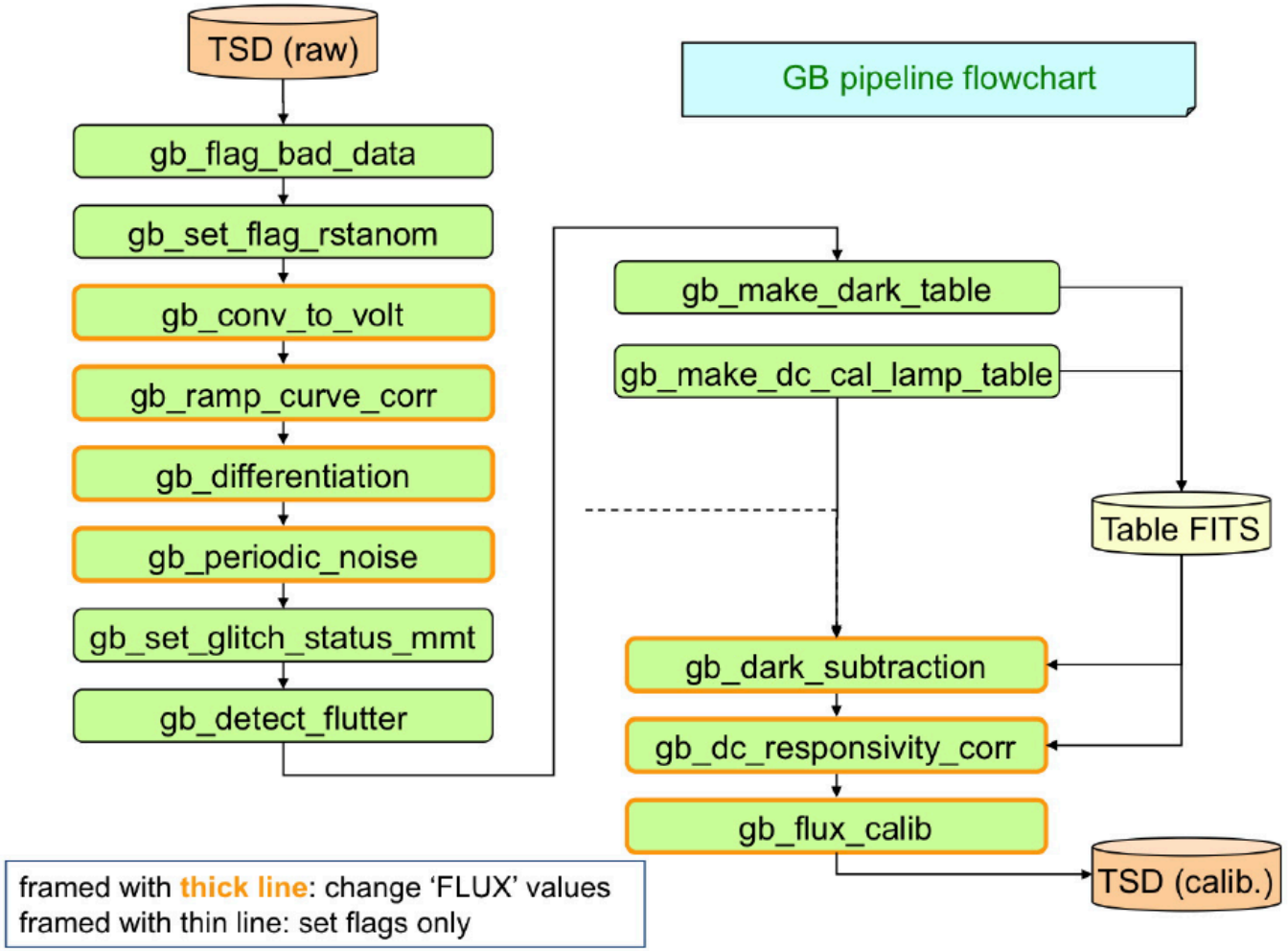

FIS Flux Calibration Strategy

	Purpose	Requirement	Timescale	Source
Internal Calibrators	Relative	Stability	< 100 min	Cal. lamps
External Calibrators	Relative	Stability Visibility	> 100 min	Stars
Absolute Calibrators	Absolute	Accurate flux	∞	Stars Asteroids

FIS Flux Calibration Strategy

	Purpose	Requirement	Timescale	Source
Internal Calibrators	Relative	Stability	< 100 min	Cal. lamps
External Calibrators	Relative	Stability Visibility	> 100 min	Stars
Absolute Calibrators	Absolute	Accurate flux	∞	Stars Asteroids

Calibration pulse signal trend (1 day)

Periodic pattern is responsivity variation by
Passage of polar-cap region (electron)
Passage of the Galactic Plane (photon)

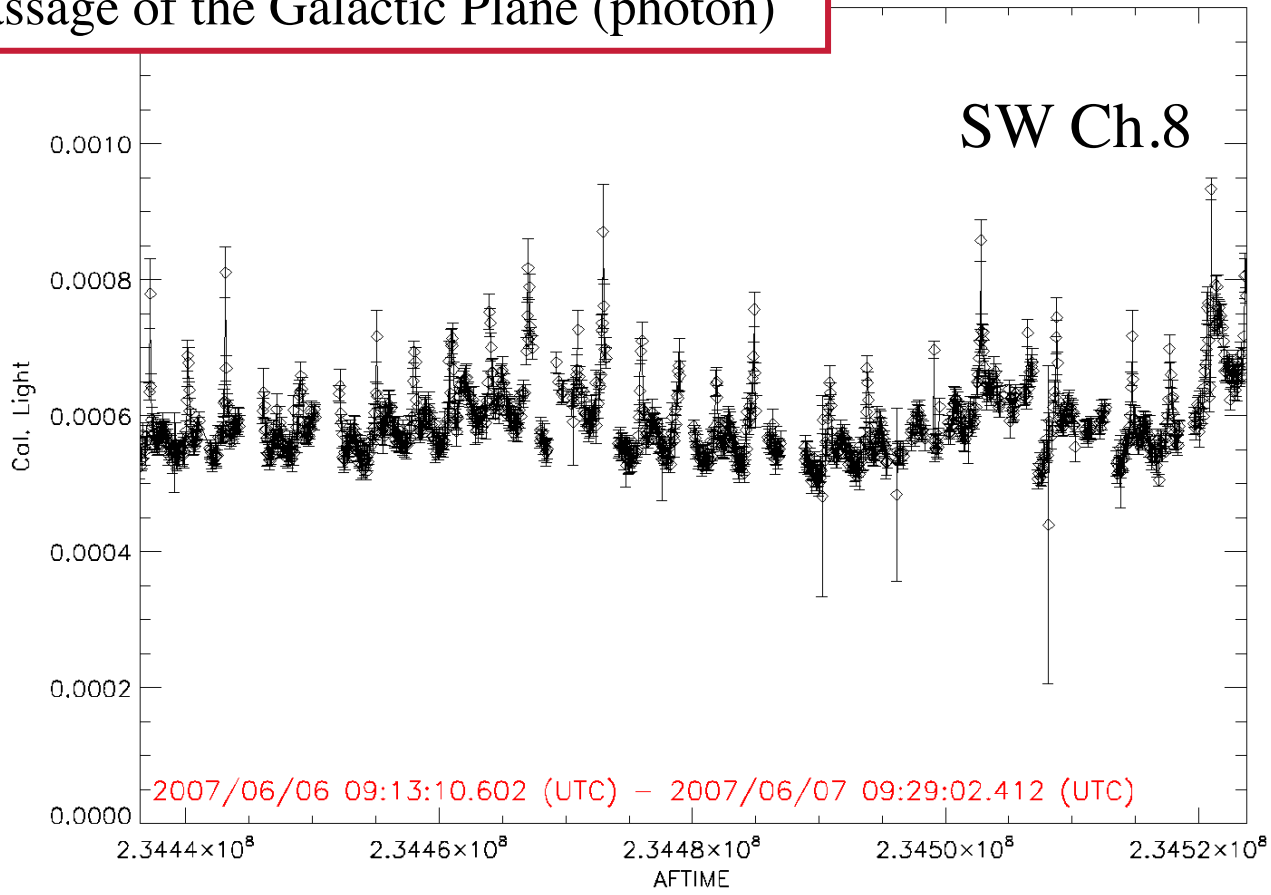

Calibration pulse signal trend (entire survey period)

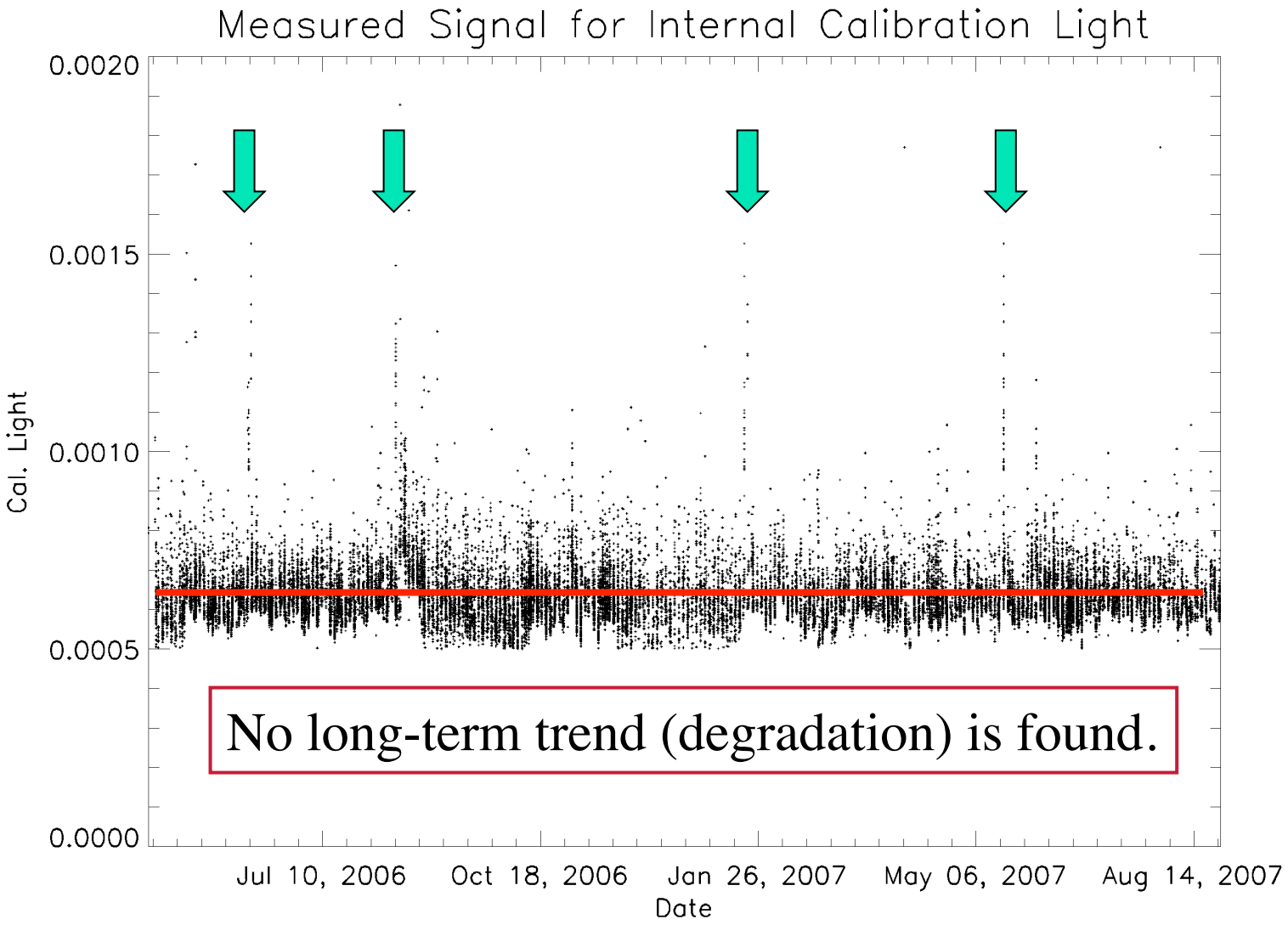

FIS Flux Calibration Strategy

	Purpose	Requirement	Timescale	Source
Internal Calibrators	Relative	Stability	< 100 min	Cal. lamps
External Calibrators	Relative	Stability Visibility	> 100 min	Stars
Absolute Calibrators	Absolute	Accurate flux	∞	Stars Asteroids

FIS Flux Calibration Strategy

	Purpose	Requirement	Timescale	Source
Internal Calibrators	Relative	Stability	< 100 min	Cal. lamps
External Calibrators	Relative	Stability Visibility	> 100 min	Stars
Absolute Calibrators	Absolute	Accurate flux	∞	Stars Asteroids

Primary calibration standards

- Asteroids
  - In-collaboration with Thomas Müller.
  - 55 candidates of flux standard asteroids are being evaluated with AKARI data.
- Stars
  - In-collaboration with Martin Cohen.
  - All-sky standard network consisting with 614 stars.
- Planets
  - Model flux provided by courtesy of Raphael Moreno.
  - Mainly for the FTS calibration.

Stellar calibrators ($F_{90} \geq 0.5$ Jy)

~110/614 sources have estimated flux larger than 0.5 Jy in WIDE-S band. They are the candidates for the FIS calibration standard.

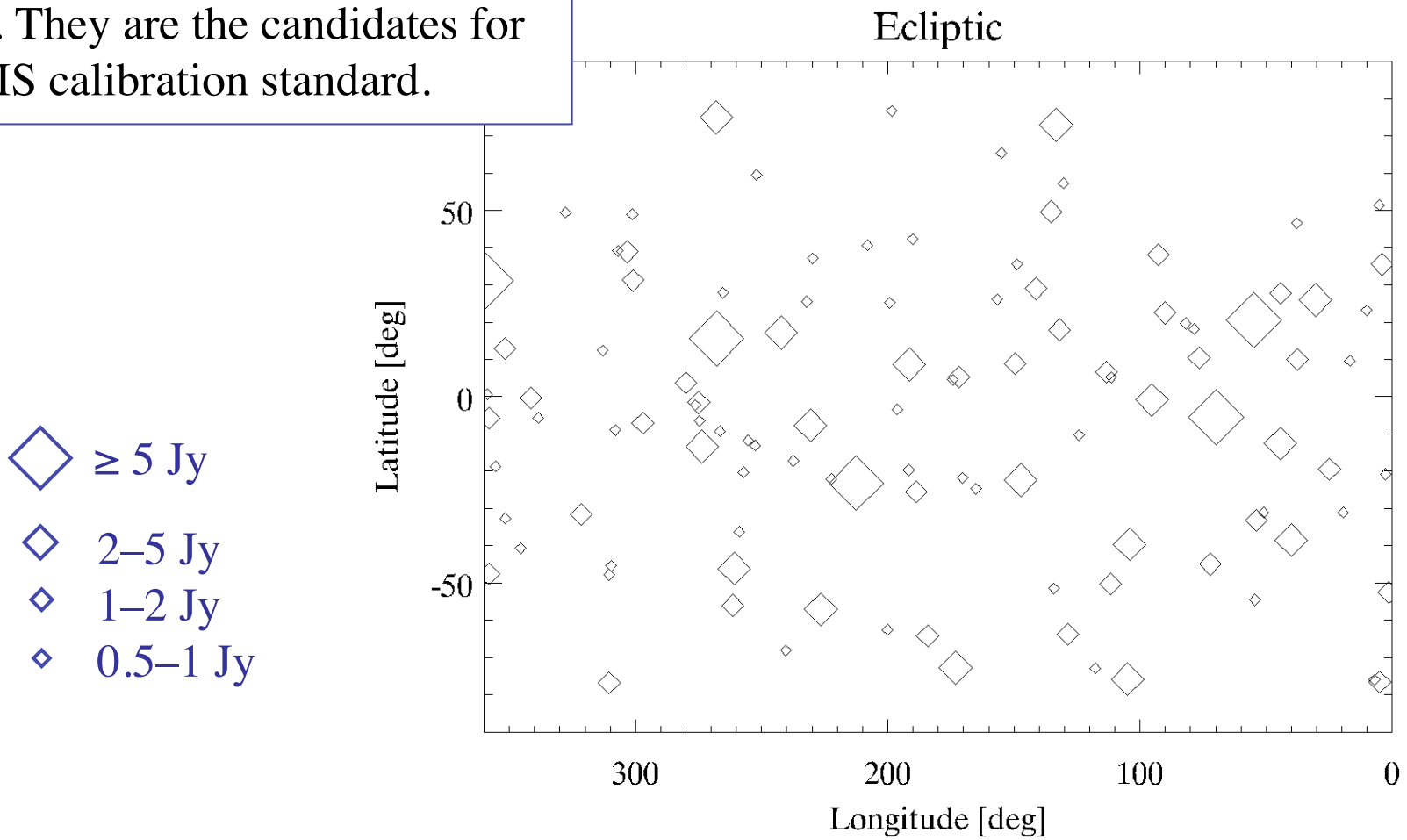

Survey observations of calibration standard asteroids and planet

- Total 228 measurements of 51 asteroid and two planets (Uranus & Neptune) during the FIS survey.

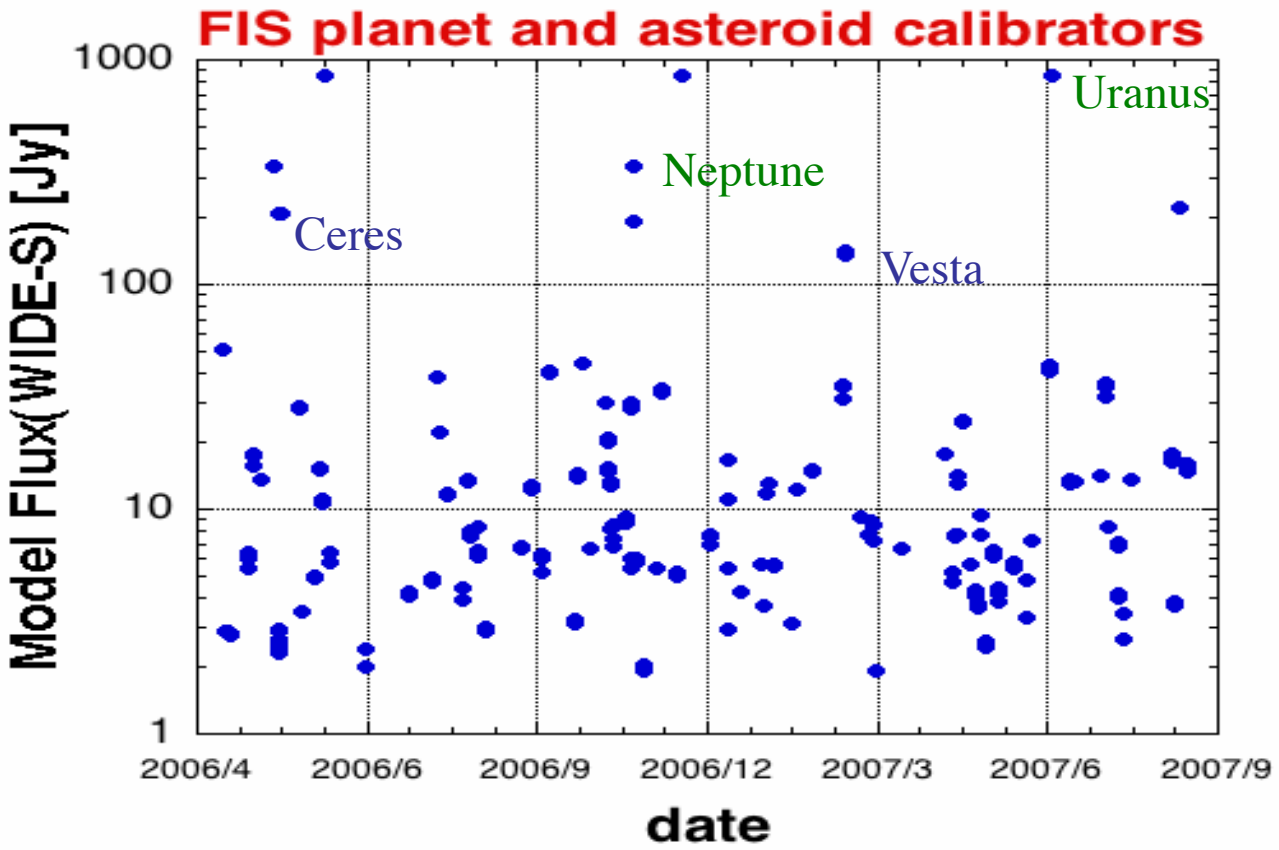

Flux measurement

- The flux quoted in the AKARI-FIS Bright Source Catalogue is measured on the co-added data from the all available scans.
  - Signals of stellar calibrators are those used for the catalogue.
  - Signals of asteroids and planets were measured on the single scan data individually.

Flux conversion factor (SW)

65 μm

90 μm

Stars / Asteroids / Planets

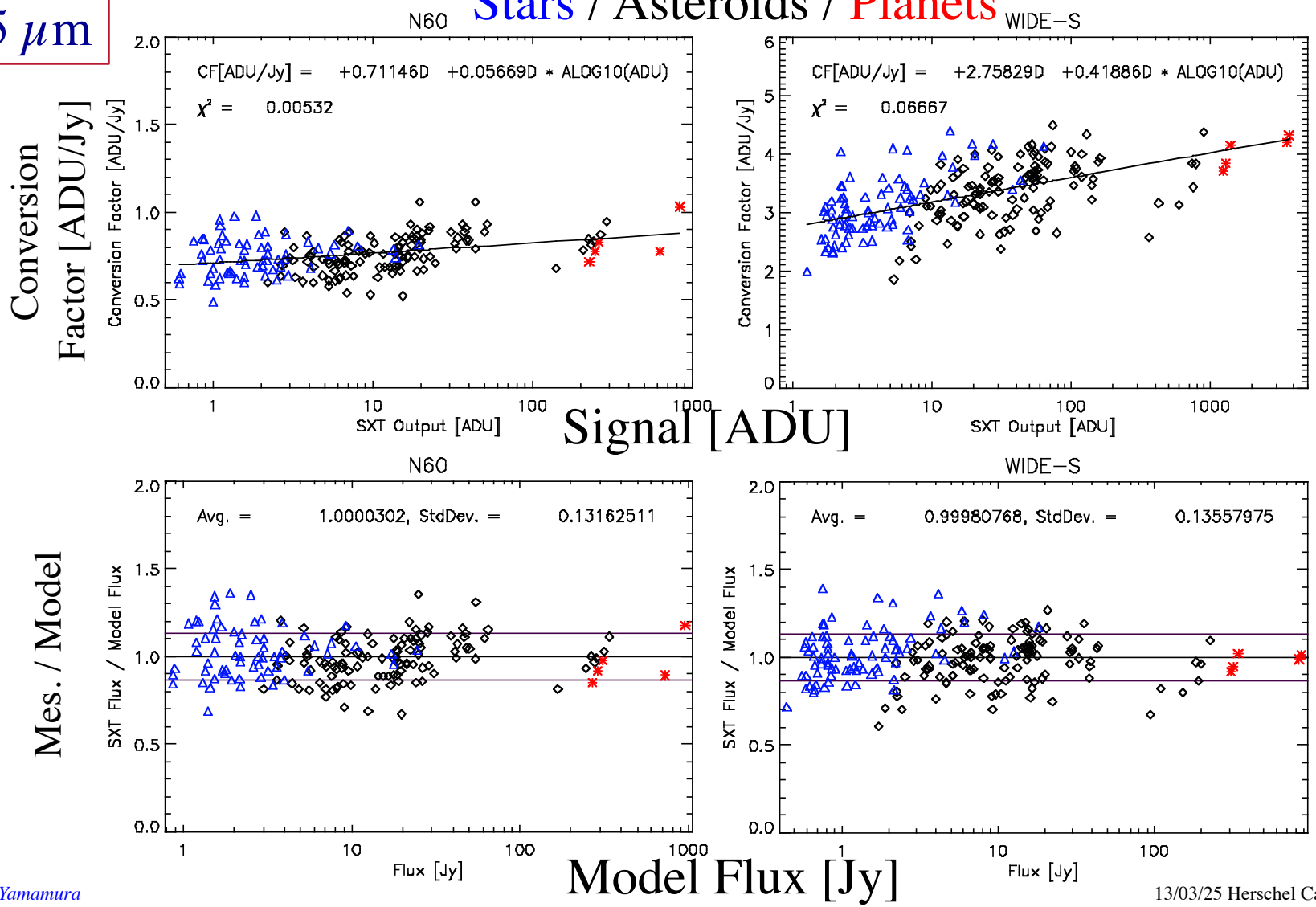

Flux conversion factor (LW)

140 μm

160 μm

Stars / Asteroids / Planets

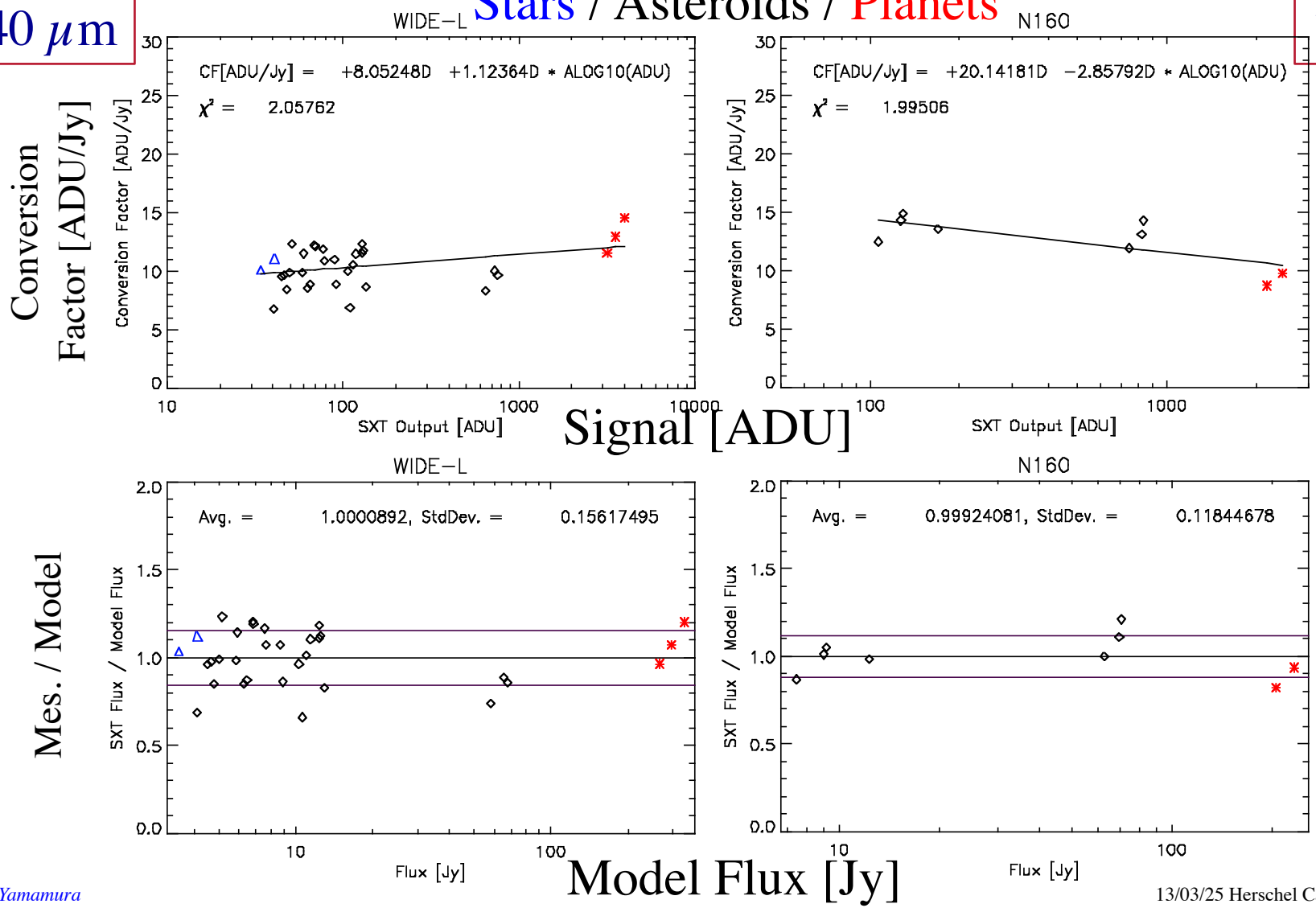

Calibration of the CDS mode data

- No observation of the calibration standard was made in the CDS mode.
- Correction function is derived by comparing the signal of the same source.

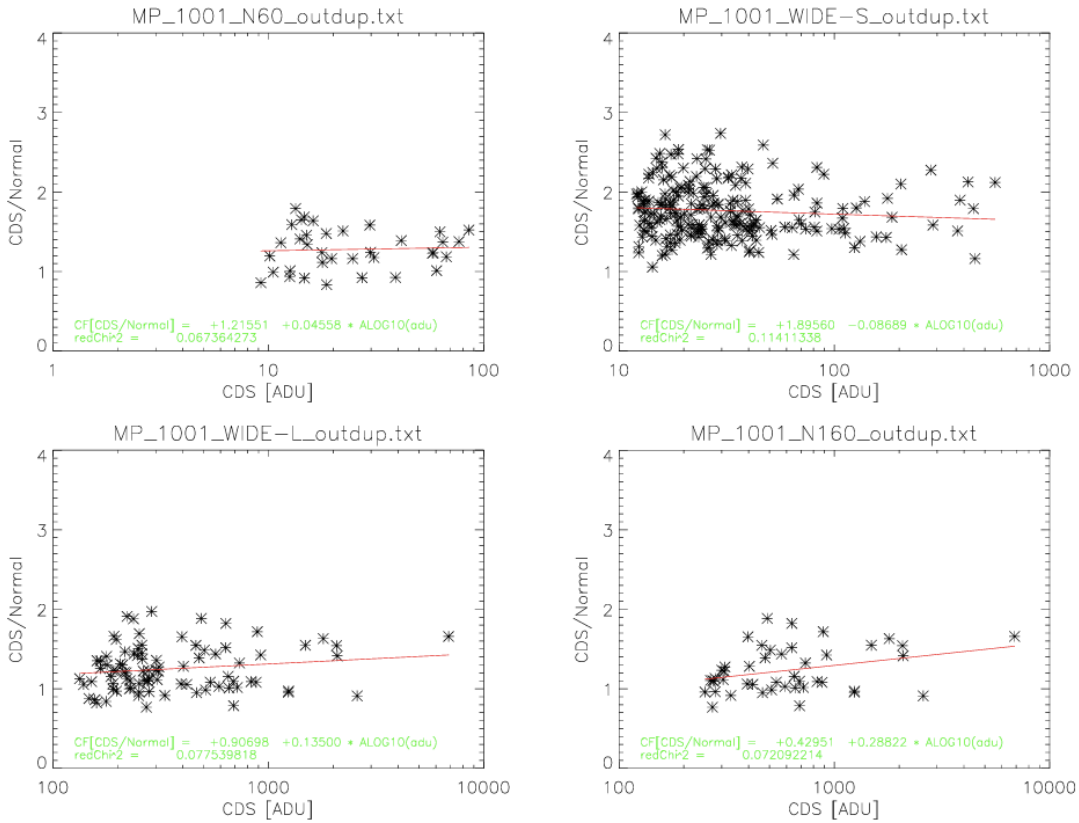

Relative flux error

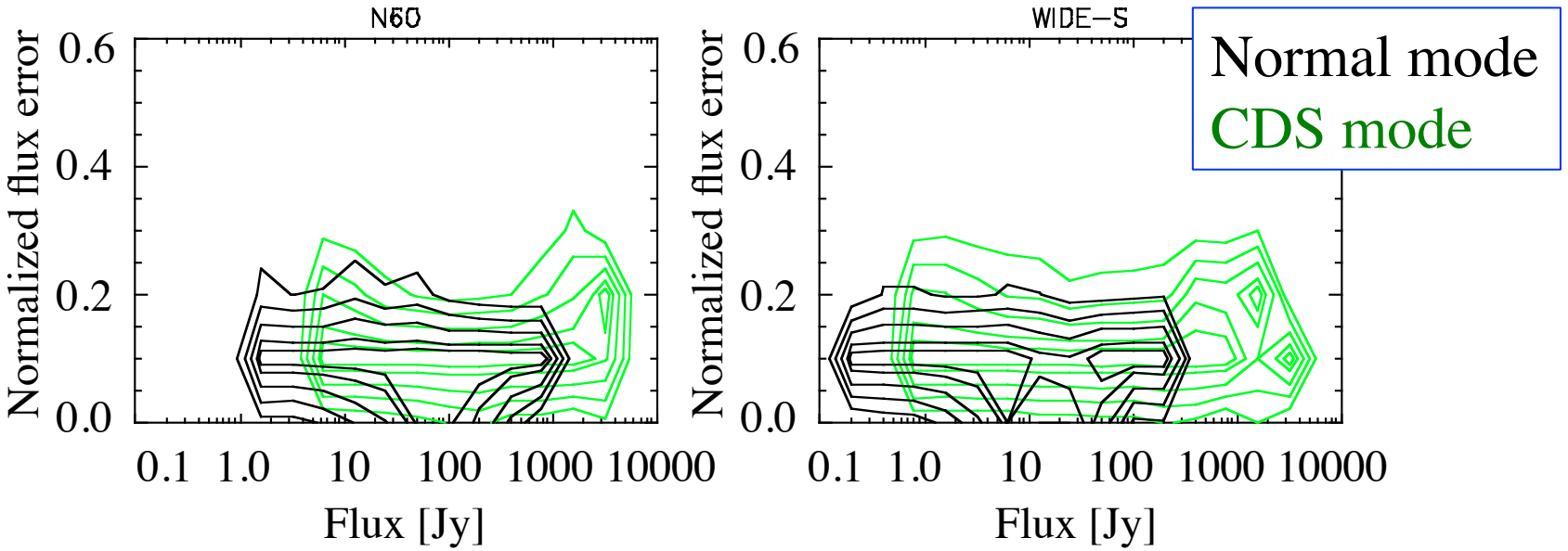

- *StdDev* of per-scan flux / coadd Flux
- Number density contour
- Majority of sources have errors of 10 % level
- Small dependency on flux level

AKARI FIS-BSC Ver.1 Release note

Flux uncertainty

- Overall flux uncertainty of the FIS Bright Source Catalogue is ~20 % for all bands.

Band	Total	Relative	Absolute
N60	20 %	10 %	15 %
WIDE-S	20 %	10 %	15 %
WIDE-L	20 %	10 %	15 %
N160	20 %	10 %	15 %

AKARI FIS-BSC Ver.1 Release note

Comparison with IRAS

- Reasonable correlation with the IRAS 60 & 100 μm fluxes.
- Deviation seen some wavelengths / flux levels is an issue of further investigation.

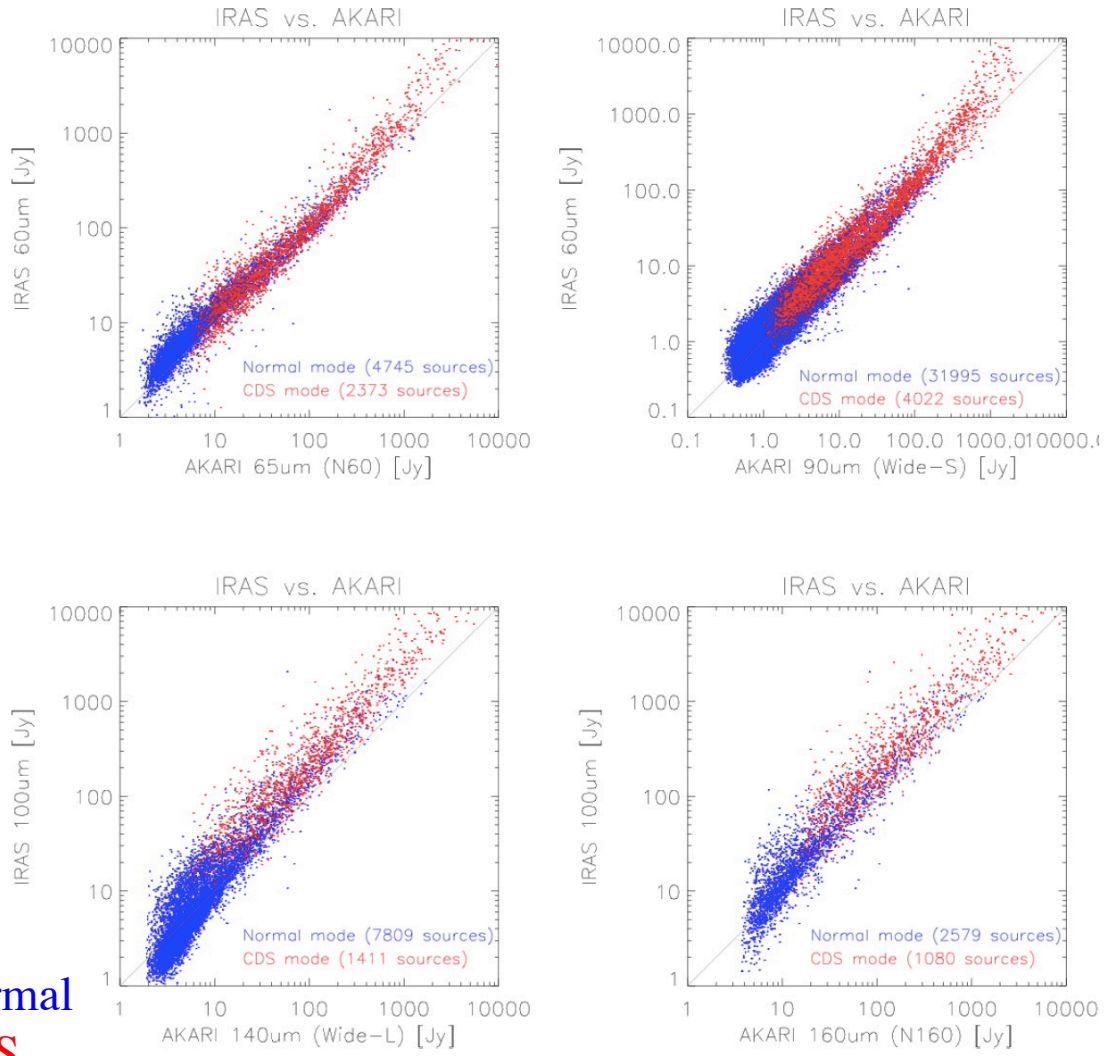

Normal
CDS

Comparison with other photometries

- FIS Bright Source Catalogue fluxes are consistent with that of FIS Slow-scan and the ISOPHOT measurements of bright galaxies.

Table 10: Comparison of flux in the BSC with that in Shirahata et al. (2009).

Band	Number of sources	Average flux ratio[1]
N60	10	1.05
WIDE-S	21	0.99
WIDE-L	5	1.02
N160	2	0.92

[1] $F_{\rm BSC}/F_{\rm Slow-scan}$.

Table 11: Comparison of AKARI/FIS fluxes with those in Klaas et al. (2001).

Band	Numbe of sources	Average flux ratio[1]
N60 / PHOT 60 μm	27	0.84
WIDE-S / PHOT 90 μm	34	0.91
WIDE-L / (est)[2] 140 μm	28	0.99
N160 / (est)[2] 160 μm	8	1.14

[1] $F_{\rm BSC}/F_{\rm Slow-scan}$.
[2] Estimated by interpolating the fluxes at the adjacent bands.

FIS BSC ver.1 Release note

FIS-BSC ver.2 & FIS-FSC ver.1

- Release schedule shifted to 2014-2015
- More sources (FSC)
- Better flux accuracy
- Better characterization
  - Detection reliability
  - Flux (small extended sources)

Calibrations of FIS diffuse map

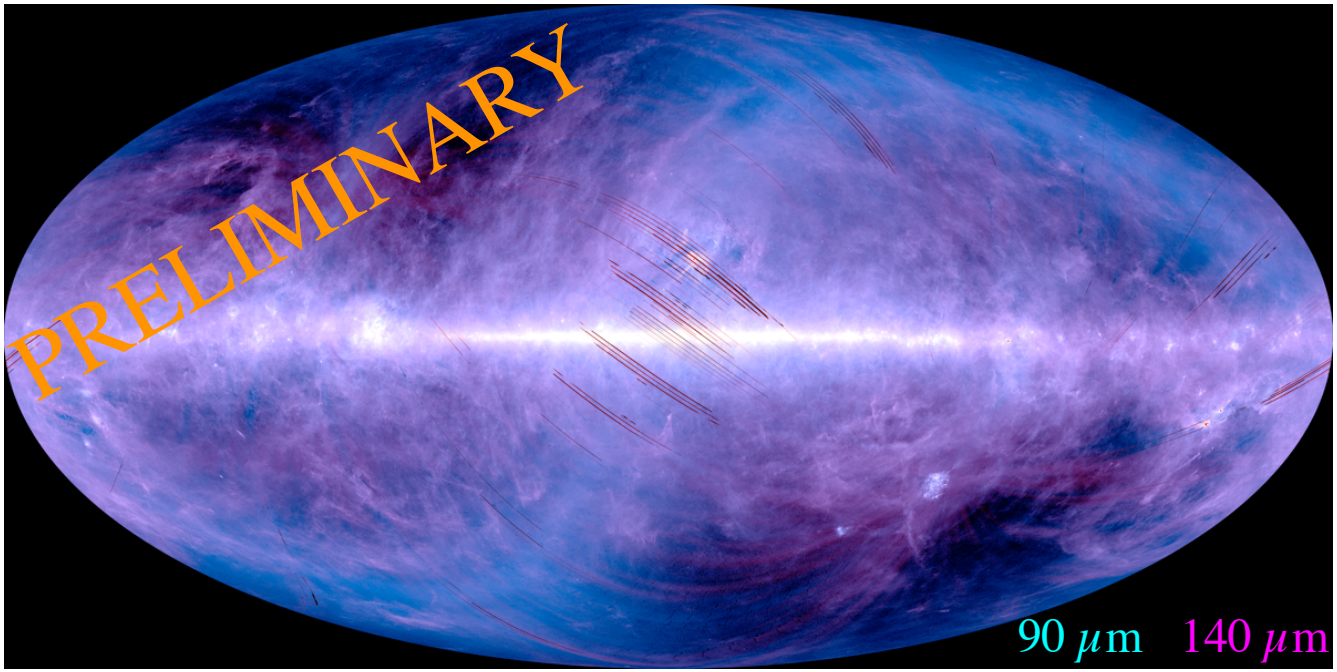

Calibrations of FIS diffuse map

- The initial flux conversion from ADU (GreenBox output) to MJy/sr is made with the gain factor derived for Slow-scan observations.
  - Pre-flight measurements with “Black body” source.
  - Comparison with the the COBE/DIRBE data in the dark sky (1–10 MJy/sr) regions.
- Uncertainties are 5% (65 μm), 5% (90 μm), 13% (140 μm), 25% (160 μm).
- Additional processing such as destriping and transient response corrections cause deviation from the real flux value. ➔ Re-calibration needed.
  - Comparison with the Slow-scan data
  - Comparison with the COBE/DIRBE data

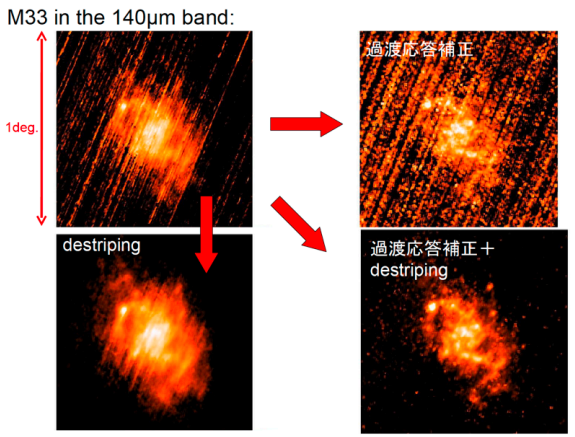

Comparison with COBE/DIRBE data

- FIS band fluxes are estimated by interpolating the DIRBE ZSMA data for every DIRBE data pixel.
- FIS image is convolved with the DIRBE beam.
- FIS and DIRBE data are compared for All-Sky data and correction factor is derived.
- These procedures are repeated. Normal and CDS mode data are treated separately

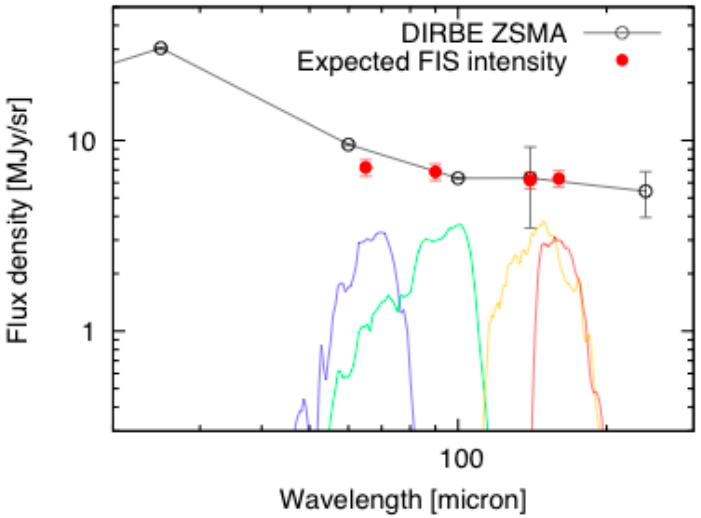

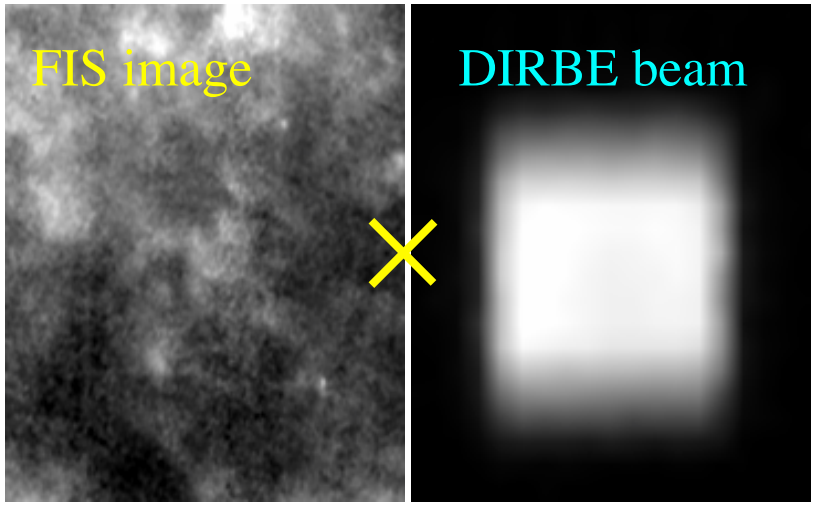

Results (current processing data)

deviation

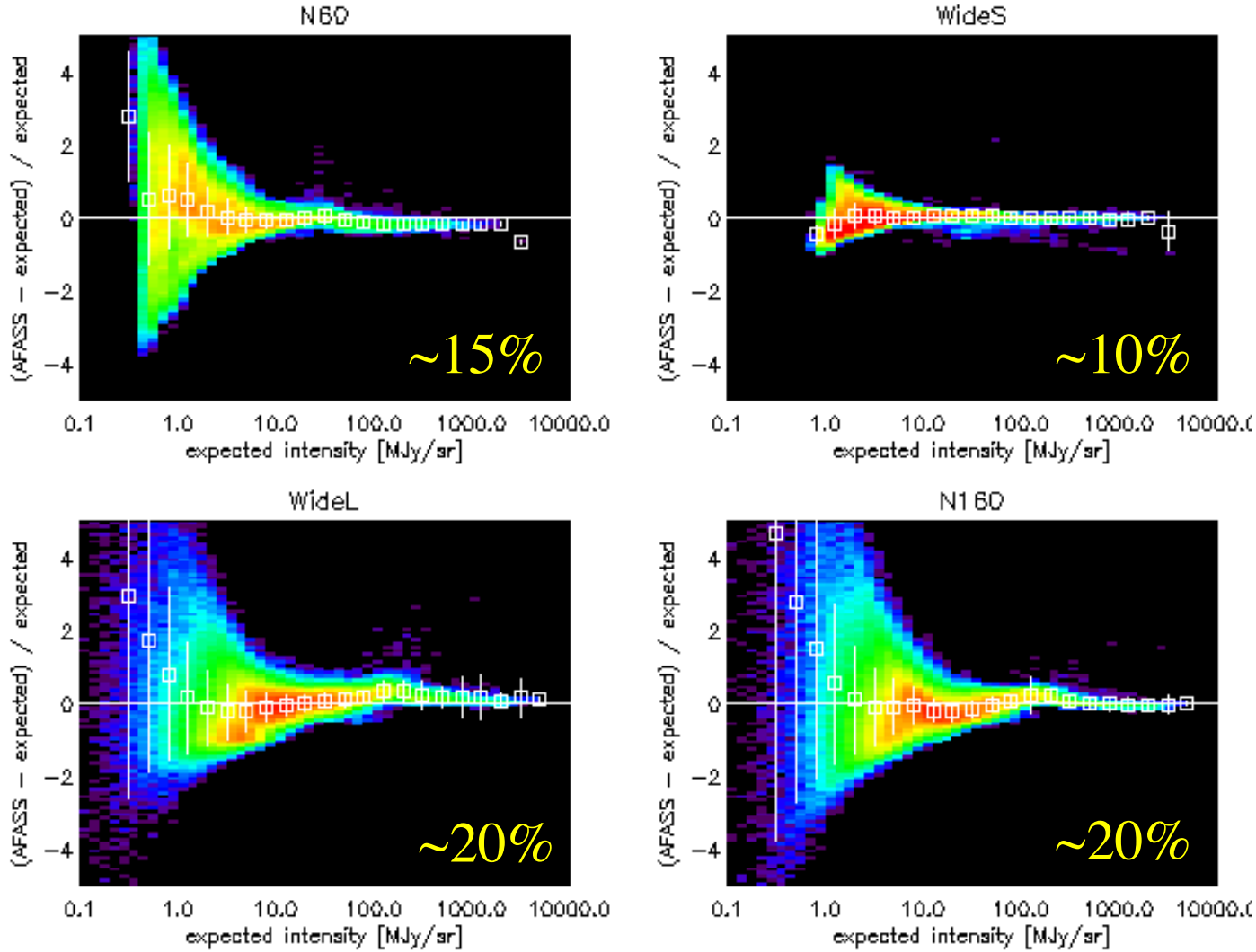

CDS/Normal gap

- Large deviations in the two LW bands at brightnesses ~200 MJy/sr ← failure of the calibration at brighter end of the Normal mode.
  - <~200 MJy/sr: Normal mode
  - >~200 MJy/sr: CDS mode

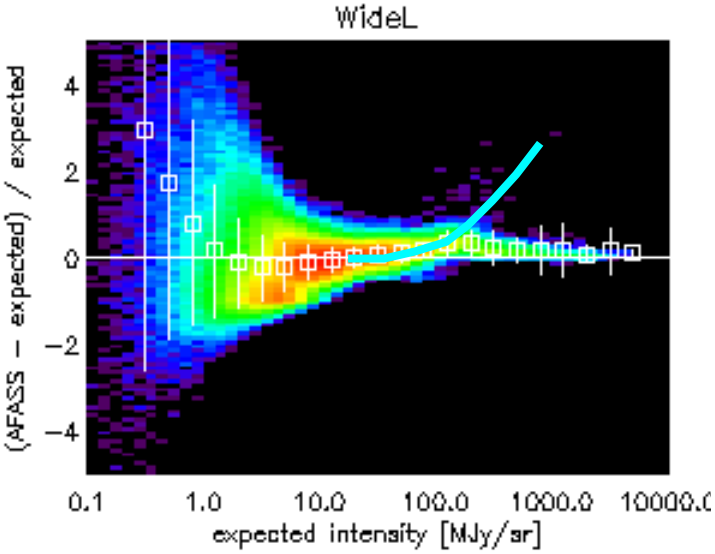

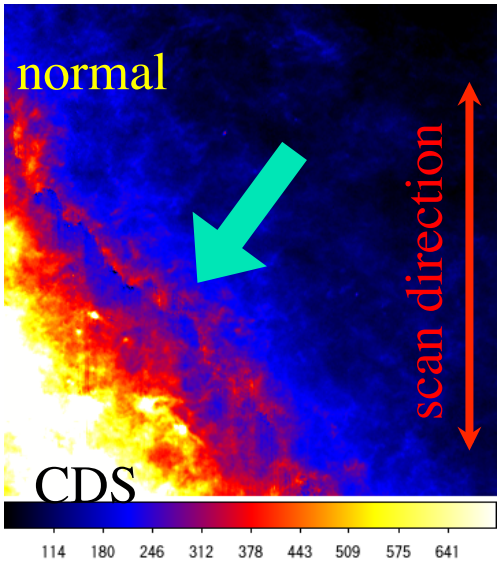

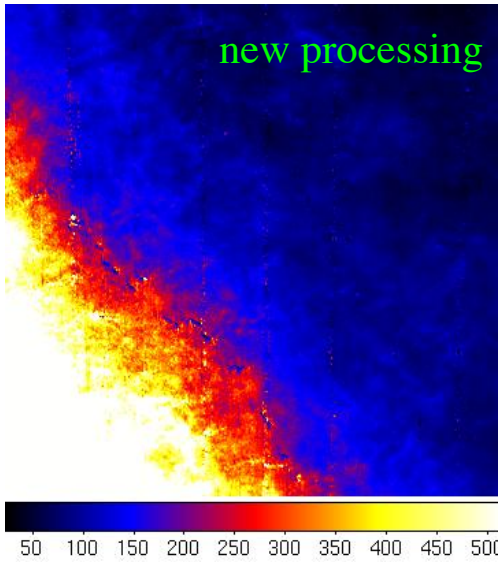

Slow-scan calibration

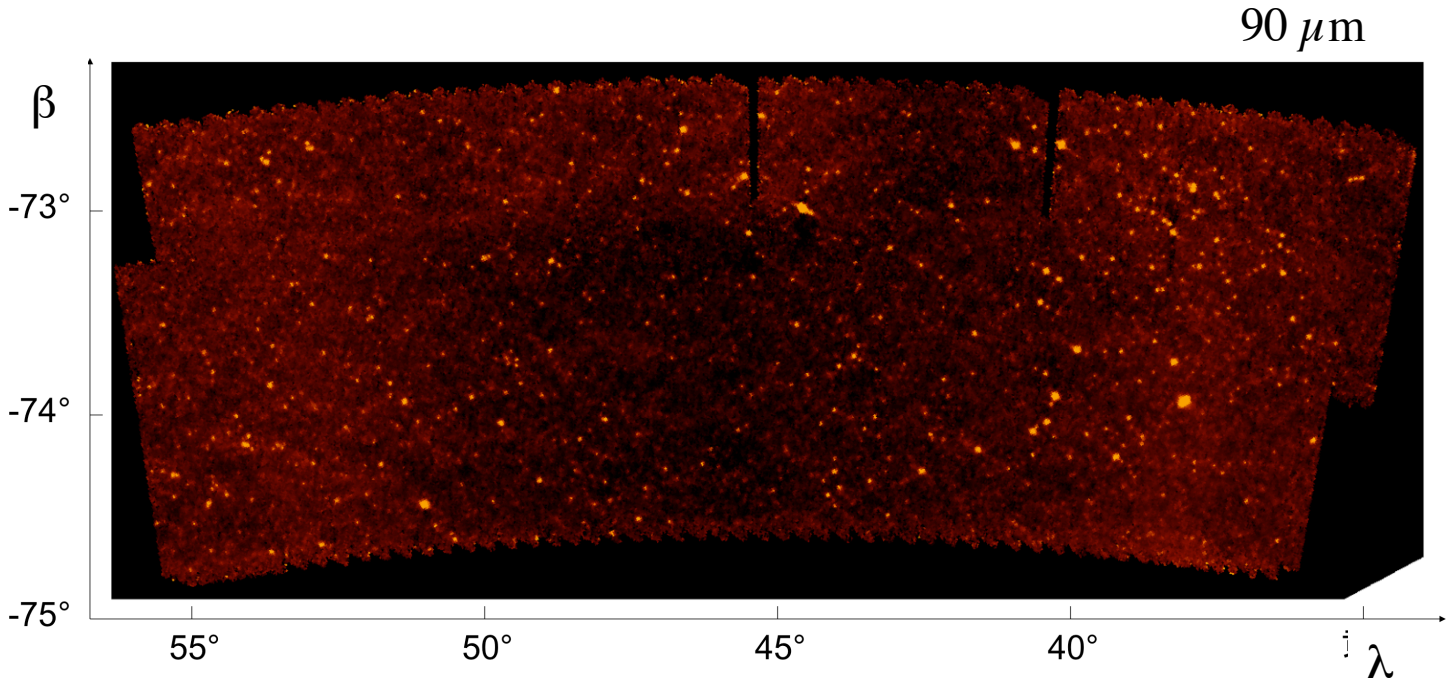

AOT FIS01

- Photometry/Mapping of small area
  - Two round-trip Slow-scan observation with a cross-scan step.
  - 10~20 x 7 arcmin^2 per obs.

- Parameters
  - Scan speed:
    - 8 or 15 arcsec/sec
  - Shift between two scans:
    - 70 or 240 sec
  - Reset Interval
    - 0.5, 1.0, 2.0 or CDS

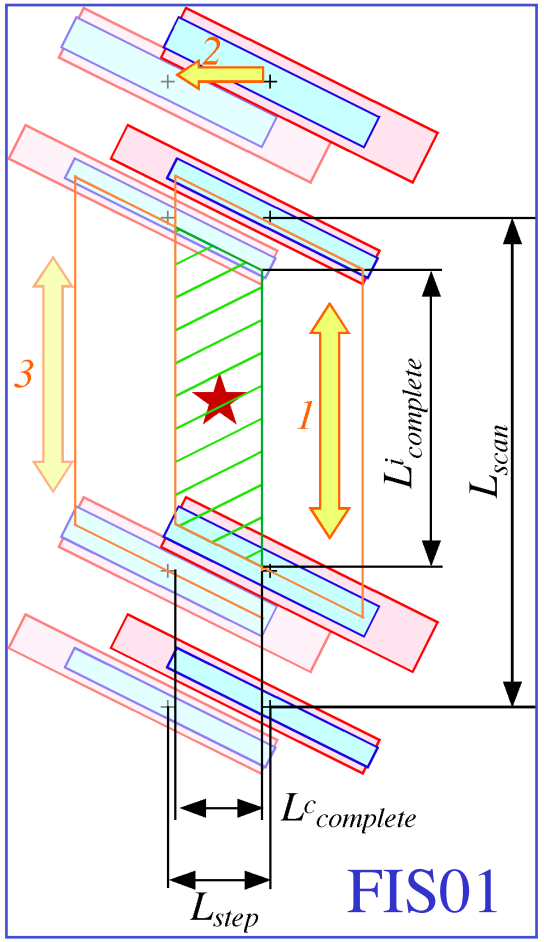

Slow-scan data example in TSD file

AOT : FIS01

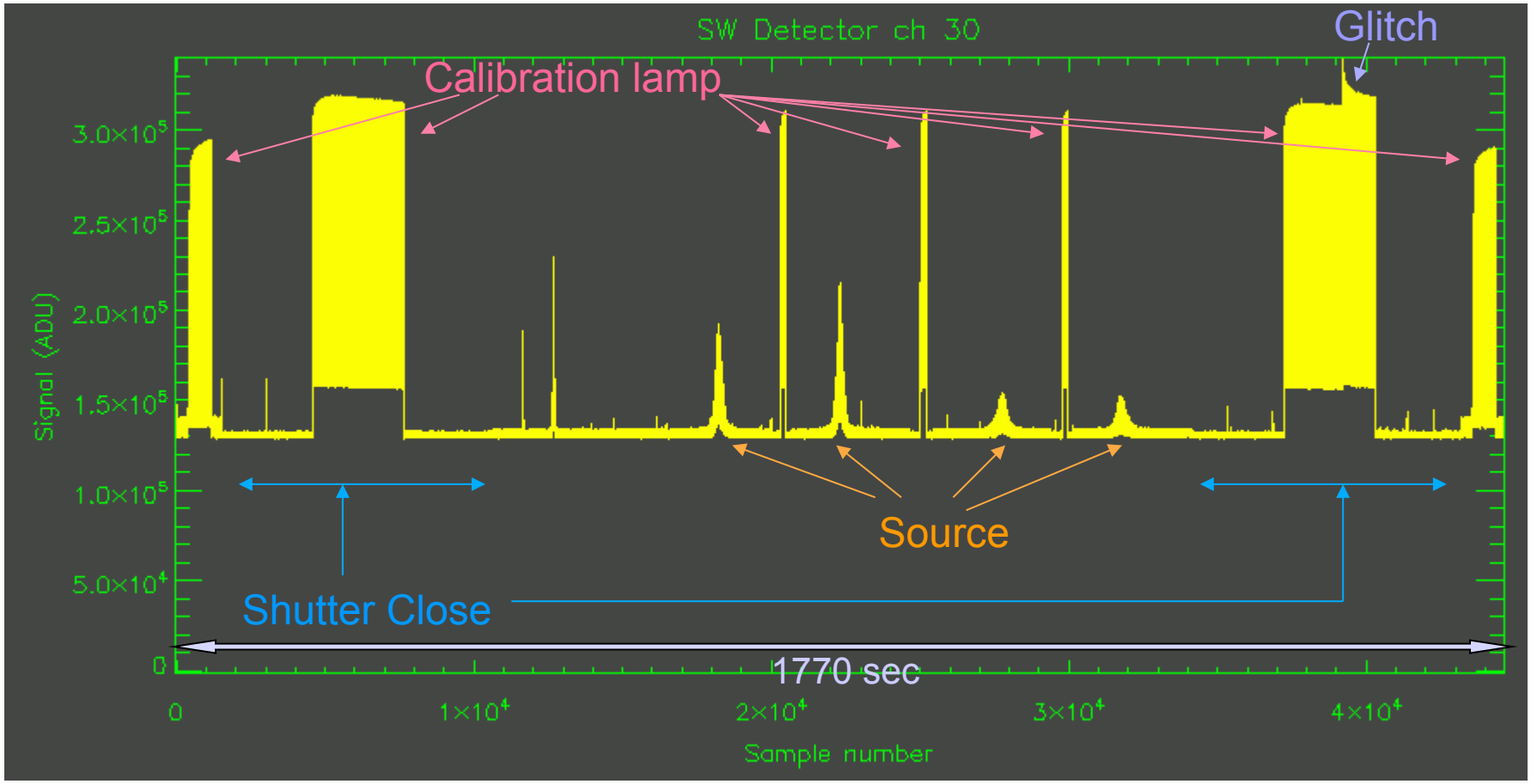

Displayed by FISv (TSD file viewer)

Pre-flight calibration

- Pre-flight measurements of the absolute gain, including detector responsivity, were carried out using an external “blackbody” source located in front of the FIS aperture.
- The temperatures ranged from 17 K to 30 K. Attenuators of 20–30 dB were used.
- The gain factors measured under different temperatures showed good agreement within ±5%.
- Internal calibrator signals were used to monitor / correct the relative variation of the detector gain. The reproducibility of the calibrator signals was approximately ±5%, and this was also the limiting factor of calibration accuracy.
- In the SW bands at 60 and 90μm, we estimated the accuracy of the pre-flight calibration to within ±7% by quadratically combining the above uncertainties.

Matsuura et al., 2011, ApJ 737, 2

Monitor Observation with NGC6543

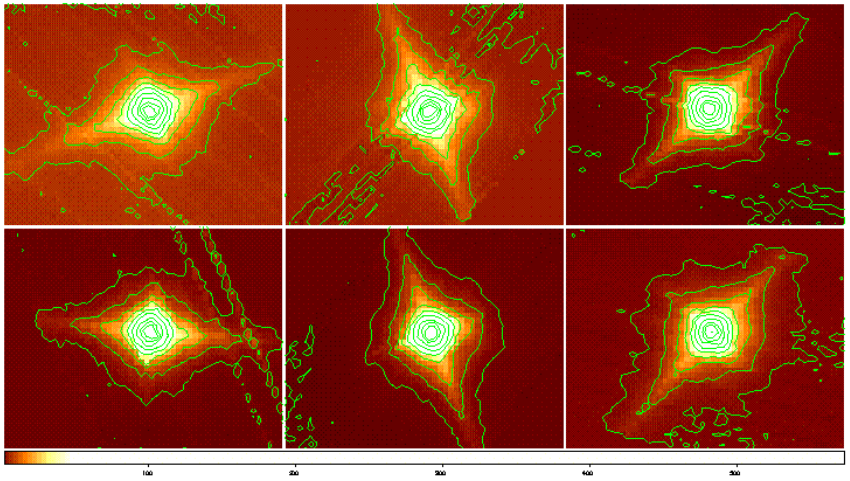

- No significant time variation is observed.

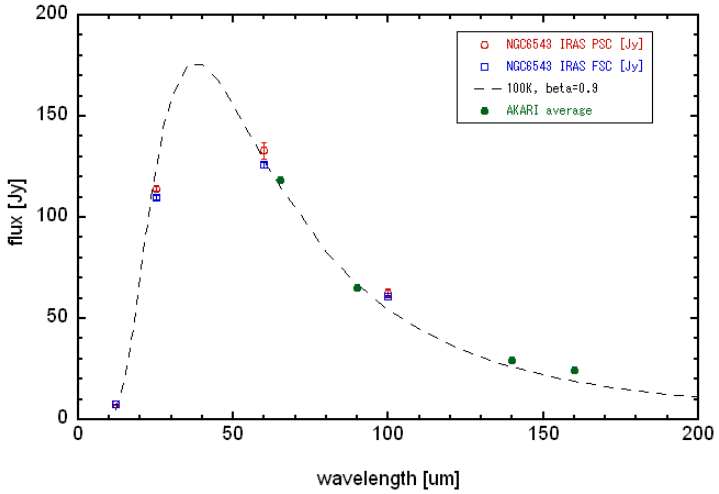

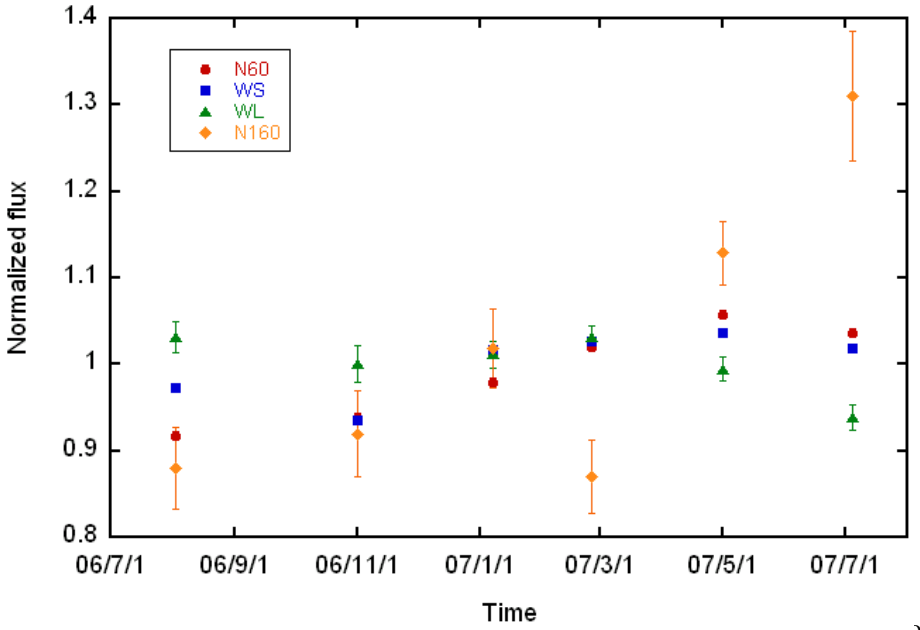

Photometry on Slow-scan image

- Point source flux measured by (e.g.,) aperture photometry on the ‘calibrated’ Slow-scan image is always lower than it must be.

- It is most likely due to the extended PSF of the instrument.

Flux standard observations

- Flux coverage: 0.1–300 Jy
- 18 obs. of 14 stars
- 17 obs. of 11 asteroids
- 2 obs. of one planet (Neptune)
- 13 obs. of 11 galaxies (for PSF mes.)

Target name	Observation		Expected flux†				
	Date	AOT parameter‡	*N60* [Jy]	*WIDE-S* [Jy]	*WIDE-L* [Jy]	*N160* [Jy]	Accuracy [%]
HR 5826	2006/04/21 20:38:35	2.0;8;70	0.338	0.237	0.064	0.052	6
HR 5321	2006/04/22 06:31:28	2.0;8;70	0.276	0.193	0.053	0.043	6
HR 5321 (2)	2006/04/22 11:28:30	2.0;8;70	0.276	0.193	0.053	0.043	6
HR 5430	2006/04/28 04:27:17	2.0;8;70	0.543	0.380	0.104	0.084	6
HR 5430 (2)	2006/04/28 06:06:18	2.0;8;70	0.543	0.380	0.104	0.084	6
HR 1208	2006/04/29 15:57:40	1.0;8;70	2.864	2.006	0.545	0.441	6
HR 872	2006/04/30 00:11:43	2.0;8;70	0.214	0.150	0.041	0.033	6
HR 872 (2)	2006/04/30 01:50:45	2.0;8;70	0.214	0.150	0.041	0.033	6
HR 1208 (2)	2006/05/02 01:43:26	1.0;8;70	2.864	2.006	0.545	0.441	6
Alpha CMa	2006/10/07 18:28:06	2.0;8;70	3.290	**2.293**	0.616	0.497	1.47
Alpha Boo	2007/01/15 00:02:26	1.0;8;70	**18.689**	**13.089**	3.558	2.879	6
Alpha Tau	2007/02/28 14:18:57	1.0;8;70	**17.042**	**11.939**	3.249	2.630	6
HD 216386	2007/06/03 01:05:46	2.0;8;70	2.177	1.524	0.414	0.335	6
HD 98118	2007/06/10 01:17:14	2.0;8;70	0.330	0.232	0.063	0.051	6
HD 222643	2007/06/11 01:23:08	2.0;8;70	0.142	0.099	0.027	0.022	6
HD 224935	2007/06/20 00:48:29	2.0;8;70	1.869	1.309	0.355	0.288	6
HD 053501	2007/07/13 02:52:02	2.0;8;70	0.175	0.122	0.033	0.027	6
HD 92305	2007/08/23 12:12:43	2.0;8;70	0.906	0.636	0.173	0.140	6
241 Germania	2006/04/27 15:44:31	0.5;8;70	8.958	**6.932**	2.356	1.940	12.5
241 Germania (2)	2006/04/27 23:59:37	0.5;8;70	7.813	**6.064**	2.073	1.707	12.5
6 Hebe	2006/04/30 03:07:09	0.5;8;70	**25.258**	**19.382**	6.469	5.313	5
6 Hebe (2)	2006/05/01 00:34:26	0.5;8;70	**25.681**	**19.699**	6.570	5.396	5
511 Davida	2006/05/02 22:50:20	0.5;8;70	**18.394**	**14.387**	4.999	4.127	7.5
511 Davida (2)	2006/05/03 12:02:32	0.5;8;70	**18.185**	**14.214**	4.933	4.071	7.5
7 Iris	2006/08/01 18:19:43	0.5;8;70	56.355	42.927	14.103	11.554	20
2 Pallas	2006/09/27 06:20:31	0.5;8;70	**59.254**	**46.375**	16.142	13.329	10
1 Ceres	2006/11/08 14:58:11	0.5;8;70	**264.848**	**206.126**	**70.786**	**58.327**	5
93 Minerva	2006/11/20 00:42:13	1.0;8;70	7.551	**5.873**	2.017	1.662	7.5
65 Cybele	2006/12/28 00:16:17	1.0;8;70	**15.192**	**11.905**	4.155	3.431	5
4 Vesta	2007/02/23 22:33:11	0.5;8;70	**200.598**	**147.871**	**44.748**	36.486	7.5
4 Vesta (2)	2007/02/24 00:12:31	0.5;15;70	**202.519**	**149.228**	**45.113**	36.778	7.5
52 Europa	2007/04/14 23:08:31	0.5;8;70	**24.150**	**18.807**	6.467	5.328	5
52 Europa (2)	2007/04/15 22:19:51	0.5;15;70	**24.328**	**18.941**	6.511	5.364	5
Neptune	2007/05/13 01:22:57	0.5;8;70	**315.942**	**361.867**	**265.605**	**248.897**	5
Neptune (2)	2007/05/13 19:36:26	0.5;15;70	**316.215**	**362.171**	**265.833**	**249.113**	5
47 Aglaja	2007/06/26 01:48:04	2.0;8;70	7.008	5.423	1.844	1.518	7.5
511 Davida (3)	2007/07/20 03:36:26	0.5;8;70	**20.743**	**16.175**	5.576	4.592	7.5

Shirahata et al., 2009, PASJ 61, 737

PSF of the FIS

- Cross-talk between the detectors is observed in the SW detector (monolithic array structure)

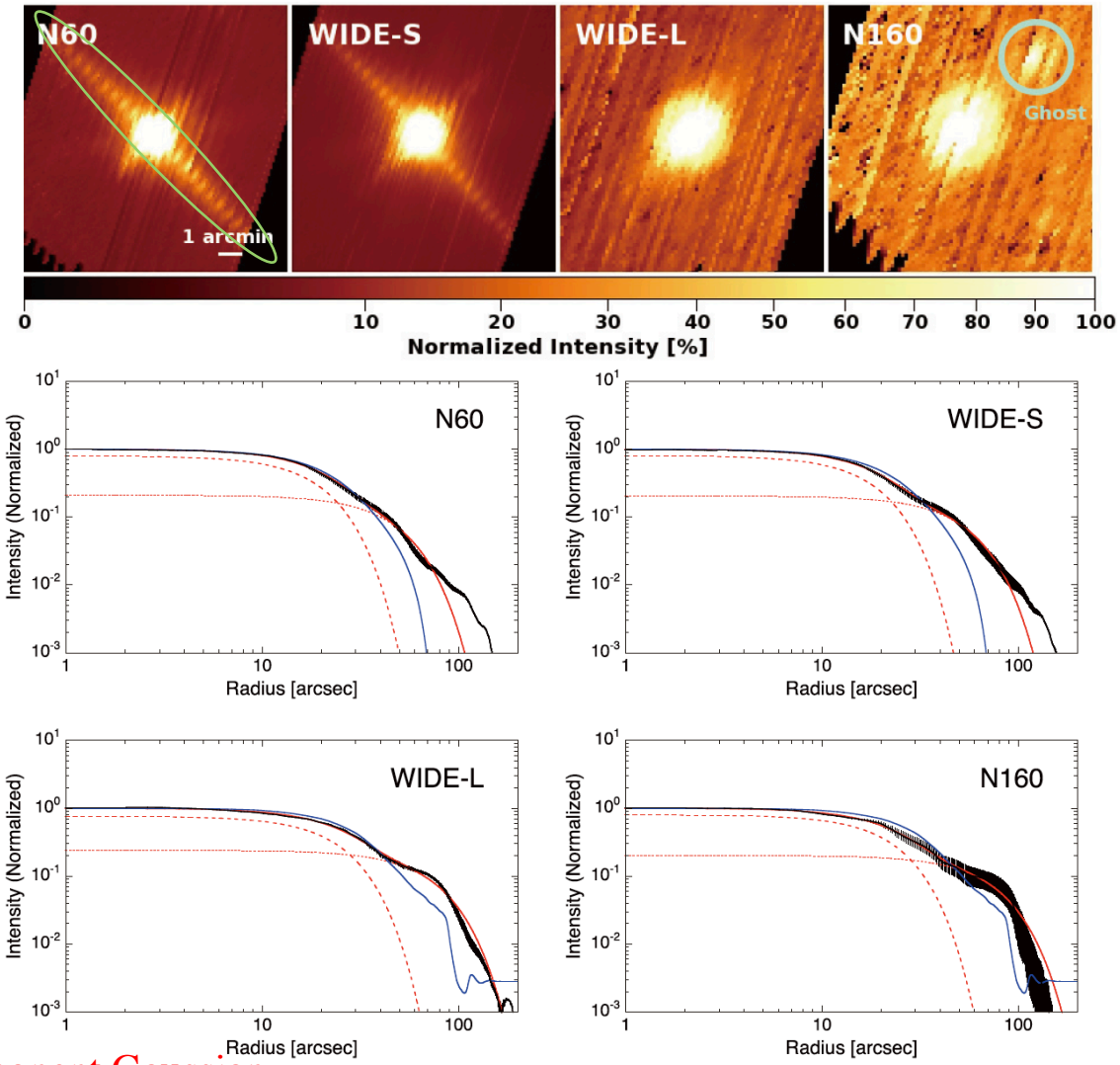

Shirahata et al., 2009, PASJ 61, 737

Flux correction factor

- The factor also depends on the total (background + source) incoming flux at 65 and 90 μm bands due to slow transient response of the detector.

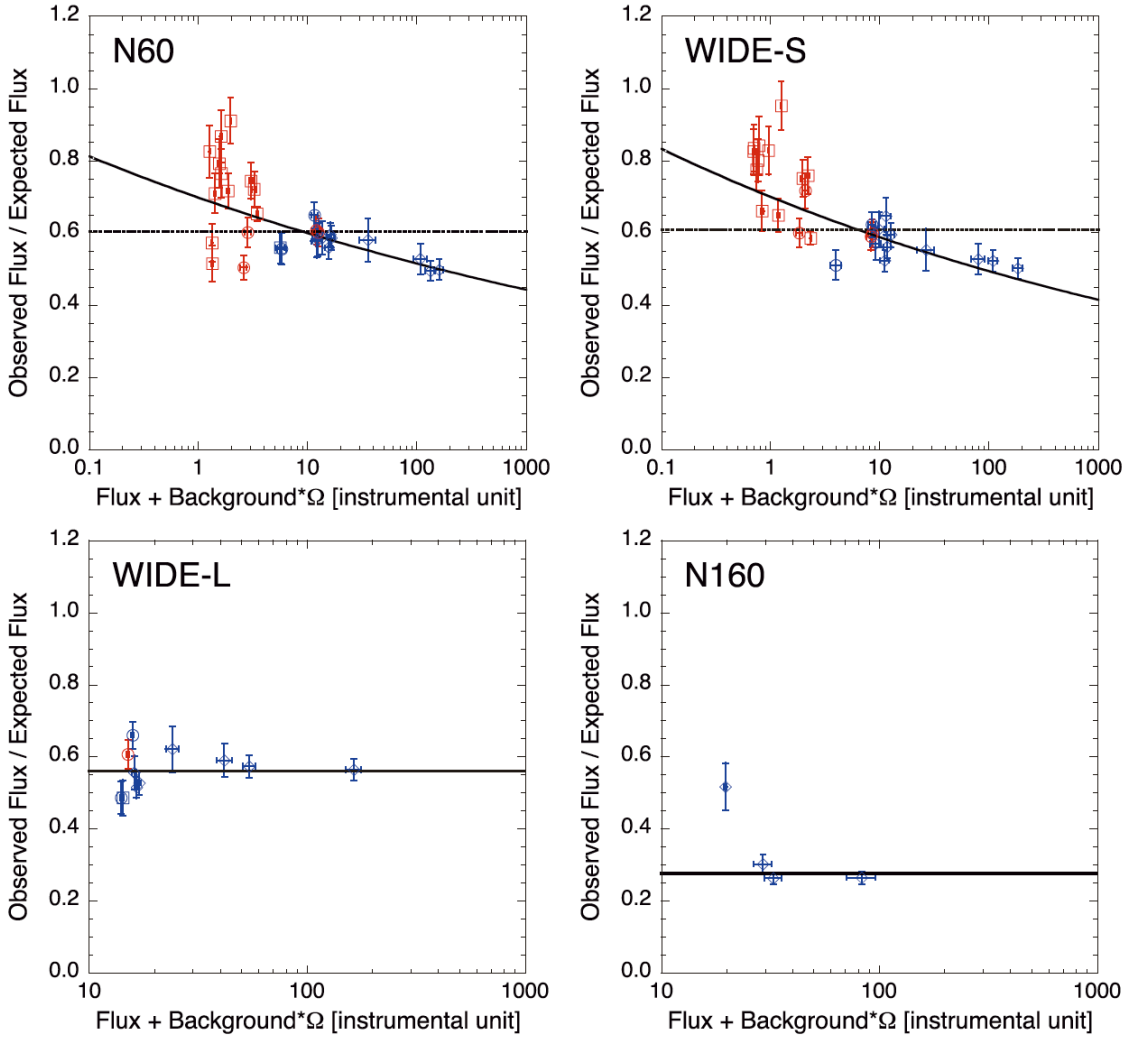

Stars
Asteroids

Shirahata et al., 2009, PASJ 61, 737

Correction factor for point source flux

Band name	Calibration factor*	Calibration accuracy [%]	Flux range† [Jy]
N60	$0.698 \times (TF)^{-0.0659}$	13.7	0.1–300
WIDE-S	$0.700 \times (TF)^{-0.0757}$	12.7	0.1–400
WIDE-L	0.560	9.97	0.5–300
N160	0.277	50.5	10 –250

* Total flux (TF) is a sum of the observed flux, background sky flux, and the detector dark current.

† Confirmed flux range. In the case of the fainter sources, the extrapolation should be possible, because the total fluxes are dominated by the detector dark current for the *N60* and *WIDE-S* bands, and the offset light signal for the *WIDE-L* and *N160* bands, respectively. The brighter end is almost comparable to the saturation limit.

Intrinsic spectrum	*N60* (65 μm)	*WIDE-S* (90 μm)	*WIDE-L* (140 μm)	*N160* (160 μm)
Black-body* ($\beta = 0$)				
- $T = 10$	4.434	1.840	1.549	1.097
- $T = 30$	1.050	0.892	0.957	0.986
- $T = 50$	0.976	0.979	0.937	0.986
- $T = 70$	0.978	1.066	0.935	0.988
- $T = 100$	0.992	1.154	0.935	0.989
- $T = 300$	1.029	1.320	0.936	0.992
- $T = 1000$	1.044	1.381	0.937	0.993
- $T = 3000$	1.048	1.398	0.937	0.993
- $T = 10000$	1.049	1.404	0.937	0.993

Large colour correction may be needed especially for WIDE-S (90 μm) band.

Shirahata et al., 2009, PASJ 61, 737

Comparison with IRAS/ISO

- 11 galaxies (used for PSF measurements)
- AKARI fluxes are consistent with IRAS / ISO within the error.

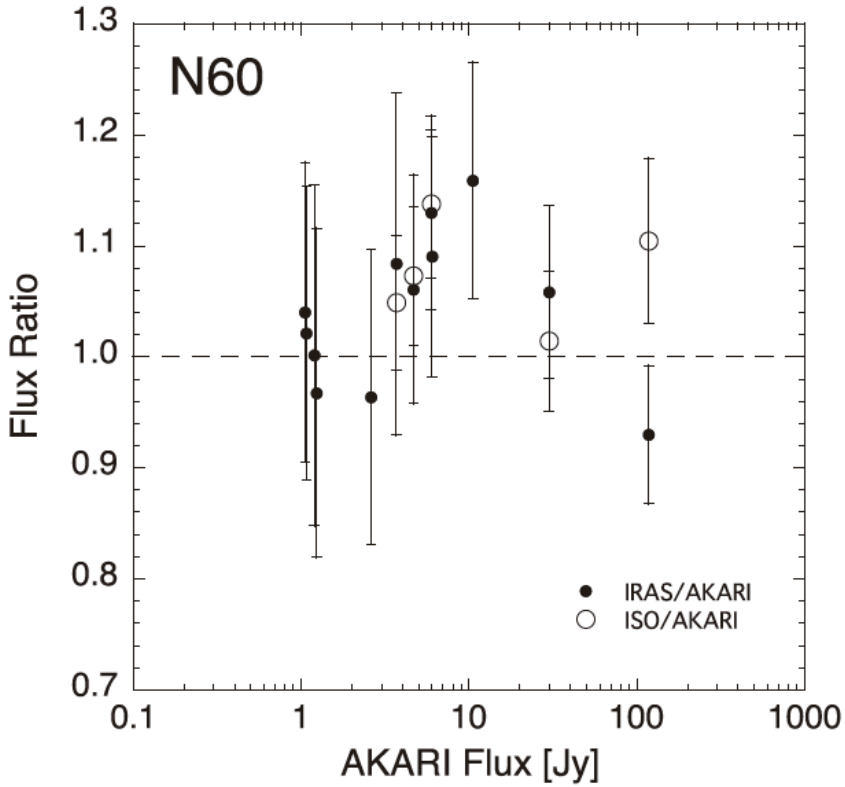

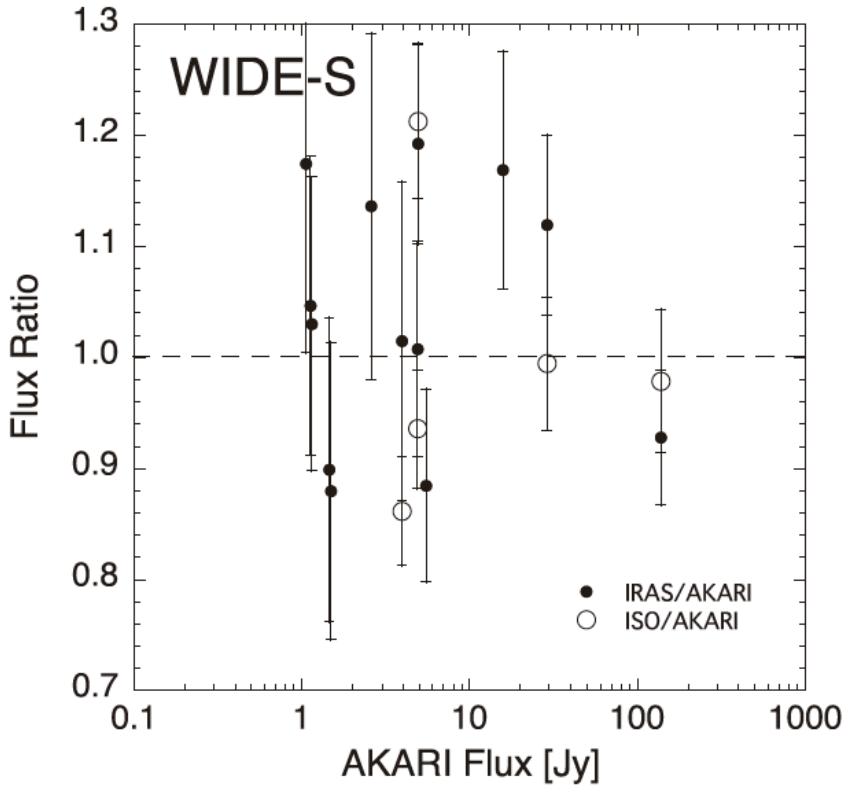

Shirahata et al., 2009, PASJ 61, 737

Position Calibration

Outline of attitude determination

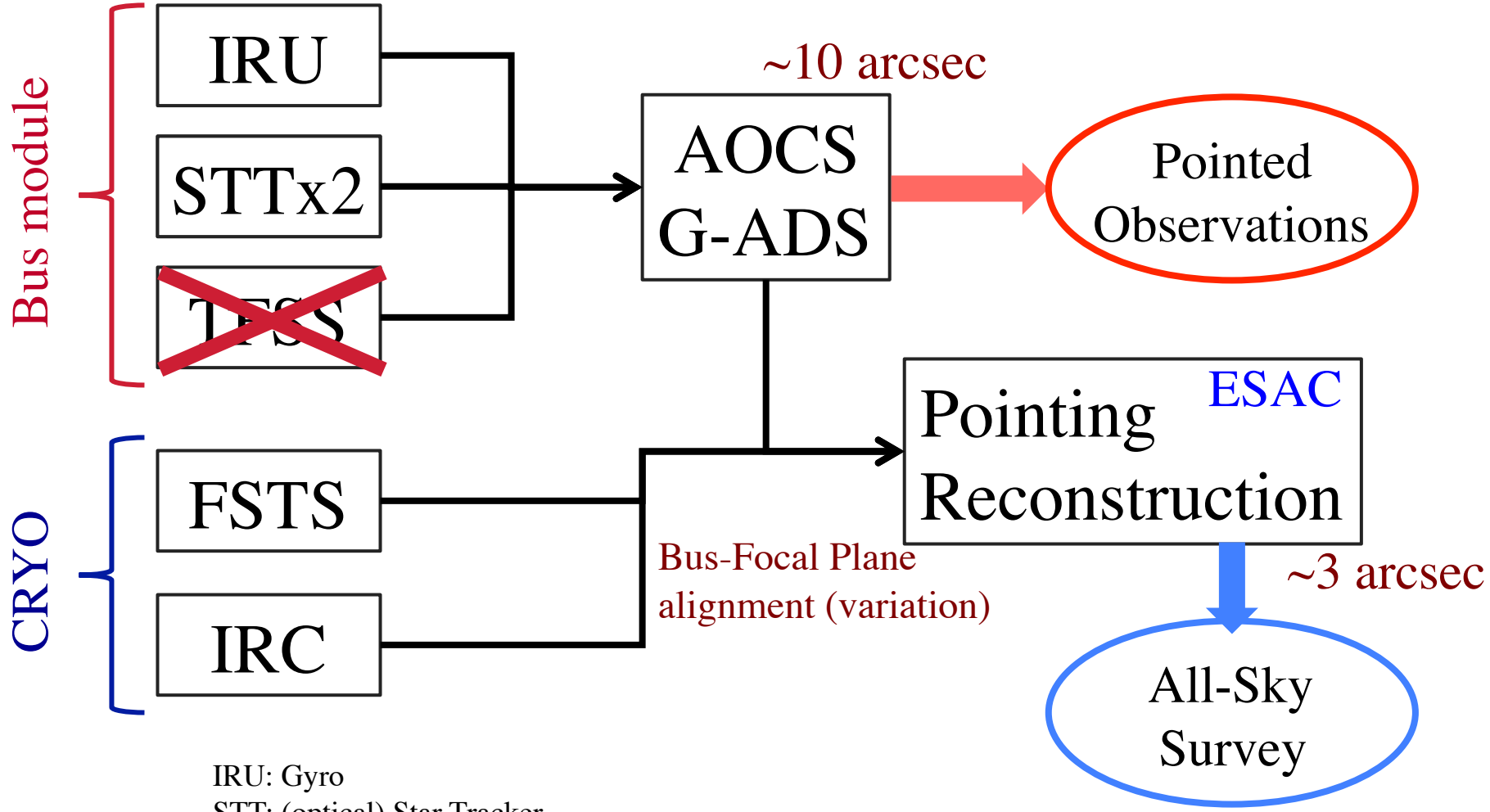

IRU: Gyro
STT: (optical) Star Tracker
TFSS: Two-dimensional Fine Sun Sensor
FSTS: Focal-plane Star Sensor
IRC: Infrared Camera

AOCS: Attitude and Orbit Control System
G-ADS: Ground-base Attitude Determination System

Pointing reconstruction

- For the regions where sufficient reference stars are detected and G-ADS output is smooth, the accuracy of the reconstructed position satisfy the requirement (in-scan: 5 arcmin, cross-scan: 8 arcmin)

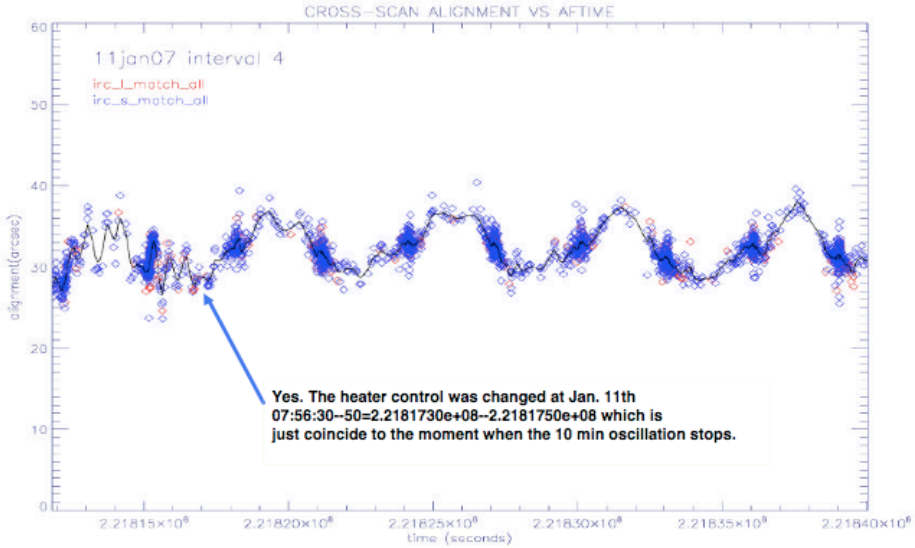

- Residual (arcsec)

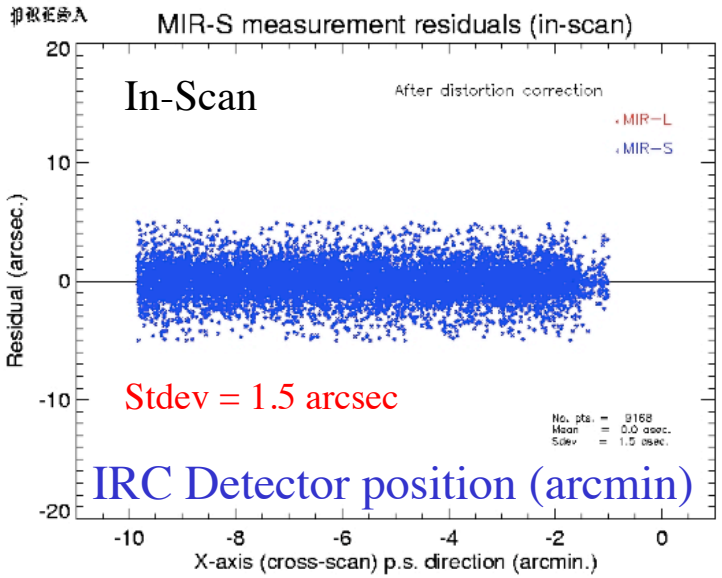

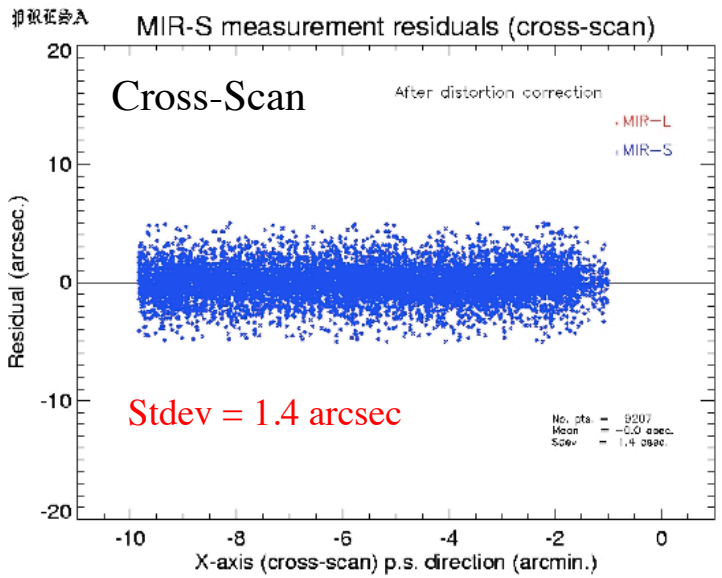

Pointing reconstruction

- FSTS (Star sensor) + IRC detection event + AOCS data
- Performed by ESAC/ESA
- Accuracy: better than 2–3 arcsec

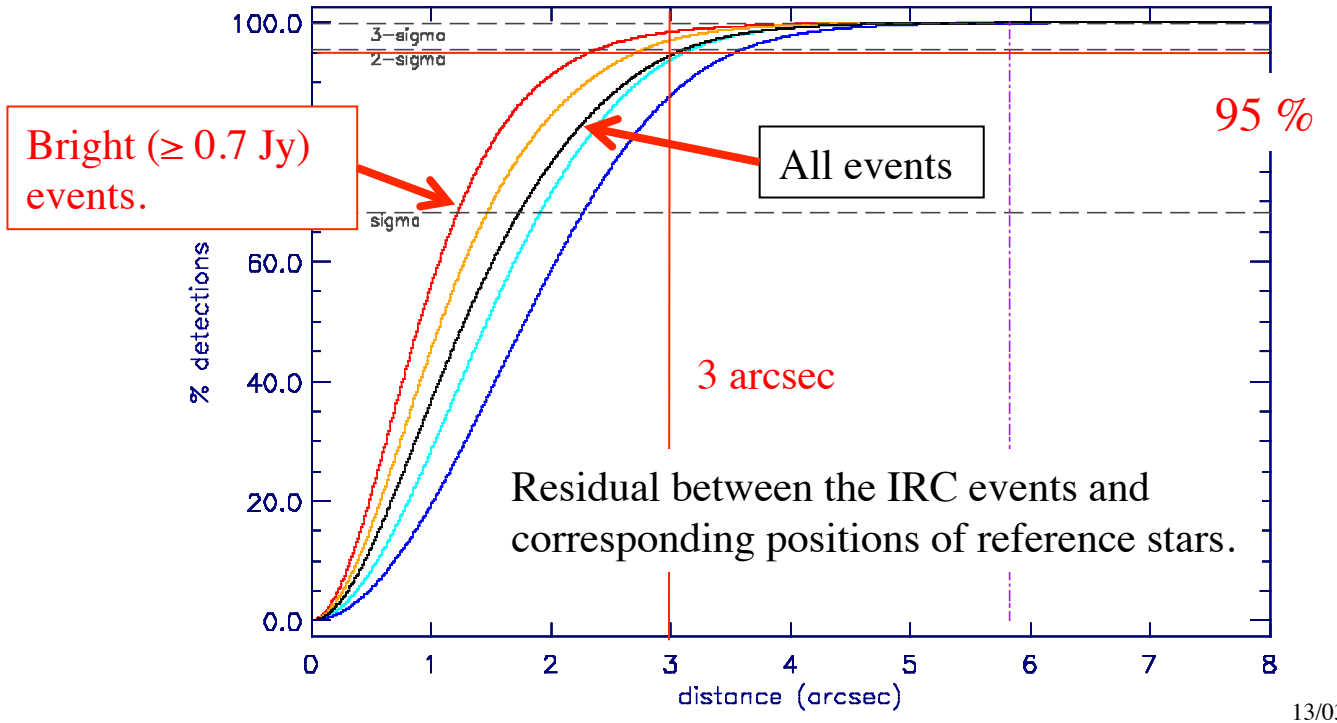

Distortion of the focal plane

- Telescope + FIS internal optics are considered to determine the projected detector pixel positions.
- Offset from boresite to the FIS detectors are determined by analysis of in-flight observing data.

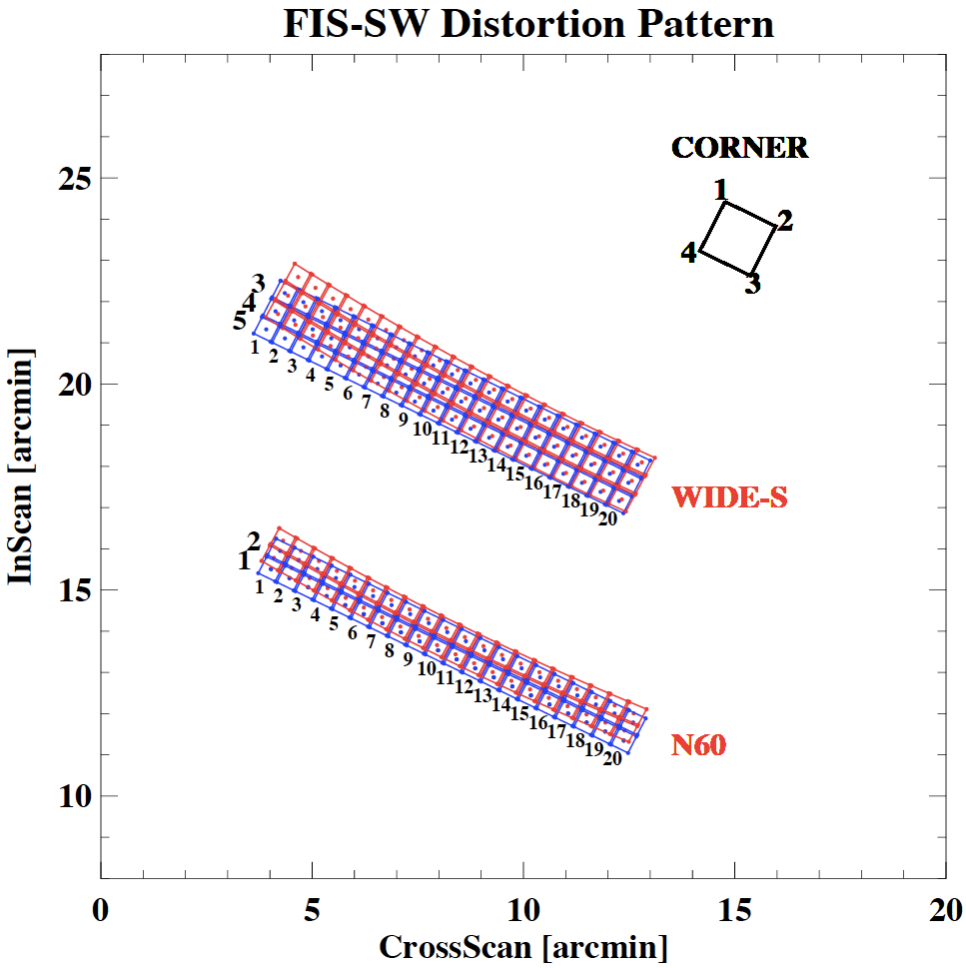

J.J. Sohn 2003–2008

FIS-BSC vs 2MASS

- At high-Galactic latitude (|b| ≥ 30 deg, LMC/SMC excluded).

$$\text{ID rate} = \frac{19184}{22843} = 84\ \%$$

- Matches are searched in 2MASS PSC within $d < 20$ arcsec.
- Found 2MASS counterpart(s) in 19184 out of 22843 sources.
- *Reversing b* w.r.t the Galactic plane resulted 5199 matches. No peak in the distance plot.

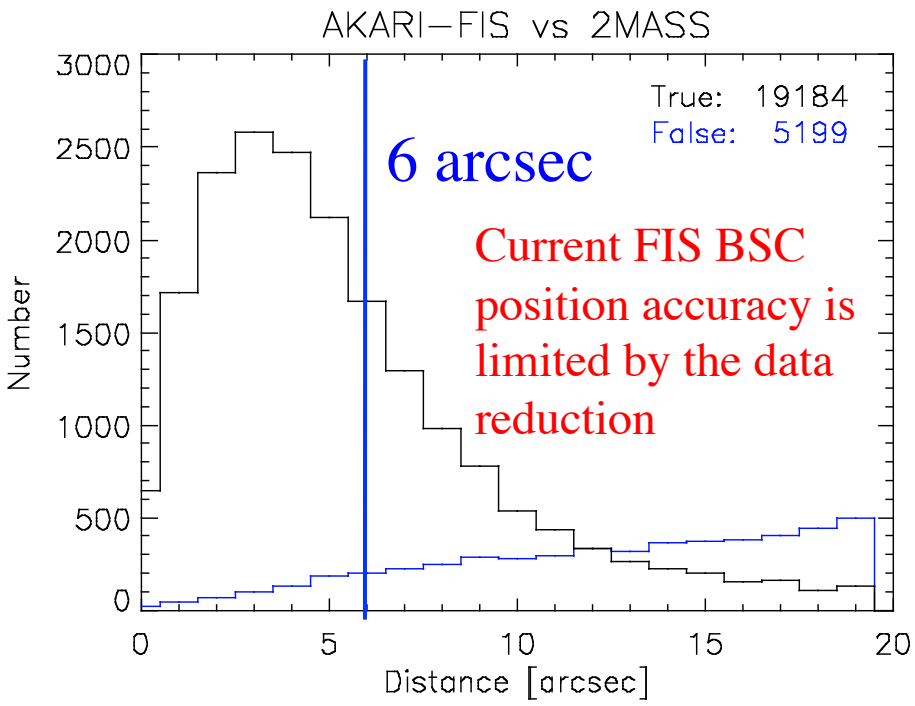

FIS-BSC vs 2MASS

- At high-Galactic latitude (|b| ≥ 30 deg, LMC/SMC excluded).

$$\text{ID rate} = \frac{19184}{22843} = 84\ \%$$

- Matches are searched in 2MASS PSC within $d < 20$ arcsec.
- Found 2MASS counterpart(s) in 19184 out of 22843 sources.
- *Reversing b* w.r.t the Galactic plane resulted 5199 matches. No peak in the distance plot.

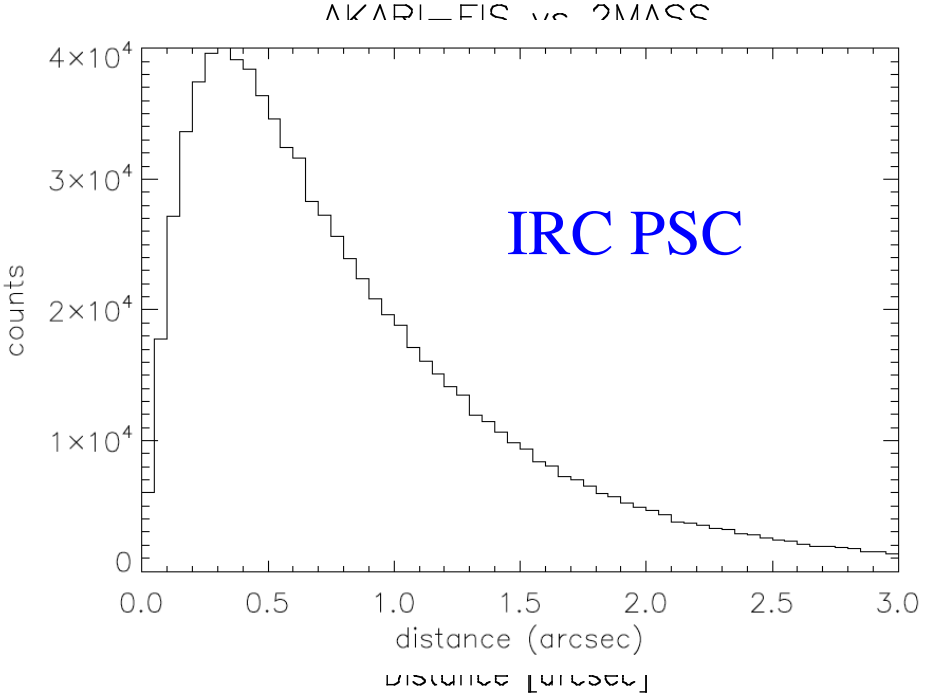

Self pointing reconstruction method

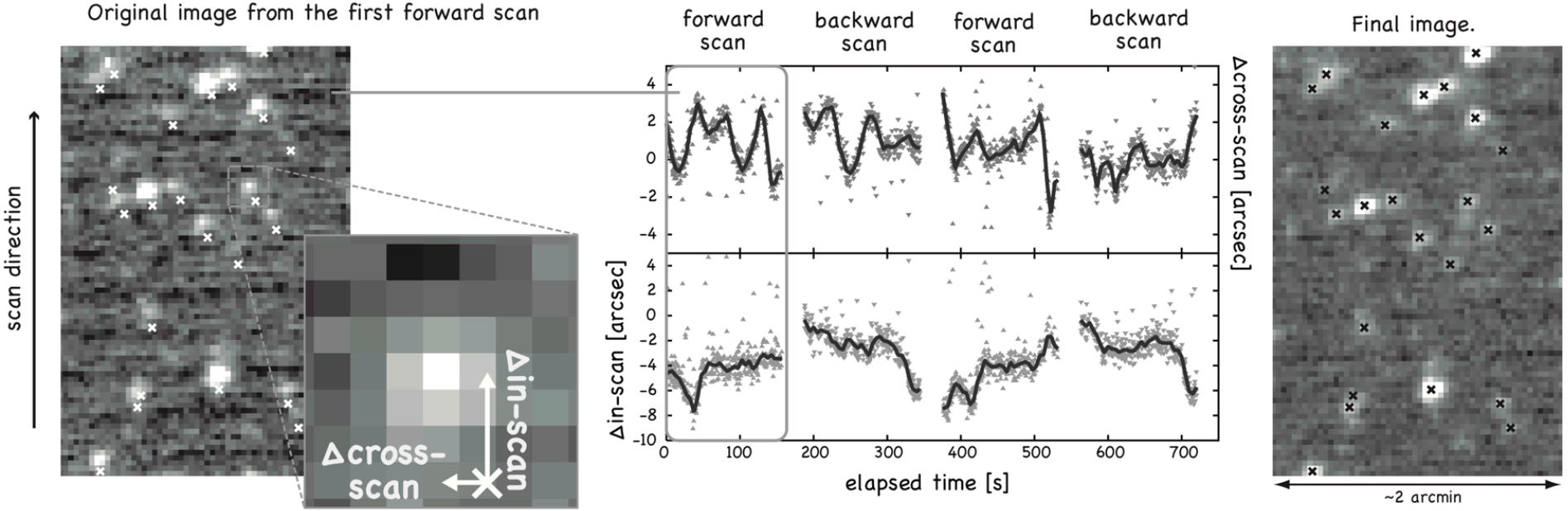

- Data reduction of slow-scan observation refers to the AOCS and GADS position data, which is as accurate as ~10 arcsec. It is not negligible especially to the IRC data of a pixel scale of 2.5 arcsec.
- Self pointing reconstruction method was developed. It works like All-Sky Survey's pointing reconstruction, comparing the position of sources detected on the MIR-S image and the 2MASS PSF.
- It improves the position accuracy as good as 1 arcsec. If the FIS slow-scan was simultaneously carried out, the result is also applied to the FIS data.

Takita et al., 2012, PASJ,

AKARI in future: New organization

- AKARI (ASTRO-F) Project will be officially closed on March 31, 2013
- A new team will start from April 1, taking over the data reduction and production of archiving data.
- The new AKARI data processing and analysis team will last five years, in which the first three years for the data production and the following two years for maintenance and archiving.
- We plan to produce revised version of the All-Sky Survey catalogues, image maps, and science ready products from the all available pointed observations.

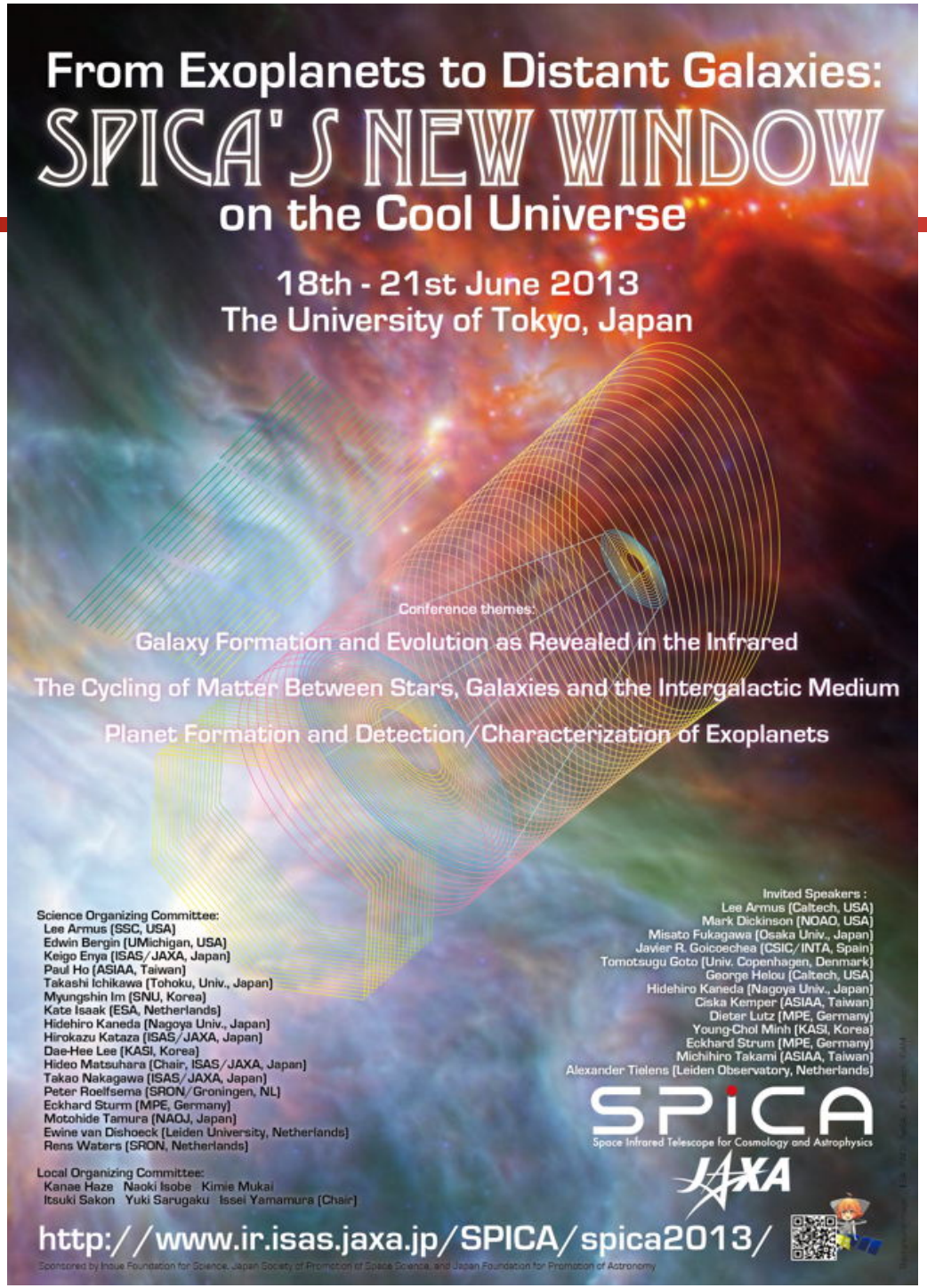
From Exoplanets to Distant Galaxies:
SPICA'S NEW WINDOW
on the Cool Universe
18th - 21st June 2013
The University of Tokyo, Japan
Conference themes:
Galaxy Formation and Evolution as Revealed in the Infrared
The Cycling of Matter Between Stars, Galaxies and the Intergalactic Medium
Planet Formation and Detection/Characterization of Exoplanets
Science Organizing Committee:
Lee Armus (SSC, USA)
Edwin Bergin (UMichigan, USA)
Keigo Enya (ISAS/JAXA, Japan)
Paul Ho (ASIAA, Taiwan)
Takashi Ichikawa (Tohoku, Univ., Japan)
Myungshin Im (SNU, Korea)
Kate Isaak (ESA, Netherlands)
Hidehiro Kaneda (Nagoya Univ., Japan)
Hirokazu Kataza (ISAS/JAXA, Japan)
Dae-Hee Lee (KASI, Korea)
Hideo Matsuhara (Chair, ISAS/JAXA, Japan)
Takao Nakagawa (ISAS/JAXA, Japan)
Peter Roelfsema (SRON/Groningen, NL)
Eckhard Sturm (MPE, Germany)
Motohide Tamura (NAOJ, Japan)
Ewine van Dishoeck (Leiden University, Netherlands)
Rens Waters (SRON, Netherlands)
Local Organizing Committee:
Kanae Haze Naoki Isobe Kimie Mukai
Itsuki Sakon Yuki Sarugaku Issei Yamamura (Chair)
Invited Speakers :
Lee Armus (Caltech, USA)
Mark Dickinson (NOAO, USA)
Misato Fukagawa (Osaka Univ., Japan)
Javier R. Goicoechea (CSIC/INTA, Spain)
Tomotsugu Goto (Univ. Copenhagen, Denmark)
George Helou (Caltech, USA)
Hidehiro Kaneda (Nagoya Univ., Japan)
Ciska Kemper (ASIAA, Taiwan)
Dieter Lutz (MPE, Germany)
Young-Chol Minh (KASI, Korea)
Eckhard Strum (MPE, Germany)
Michihiro Takami (ASIAA, Taiwan)
Alexander Tielens (Leiden Observatory, Netherlands)
SPICA
Space Infrared Telescope for Cosmology and Astrophysics
JAXA
http://www.ir.isas.jaxa.jp/SPICA/spica2013/